

MINISTERE DE L'ENSEIGNEMENT SUPERIEUR ET DE LA RECHERCHE SCIENTIFIQUE

UNIVERSITE MOHAMED KHIDER BISKRA

Faculte des sciences exactes et

Des sciences de la nature et de la vie

Département des Sciences de la matière

THESE

Présentée par

Houmam BELAIDI

En vue de l'obtention du diplôme de :

Doctorat en chimie

Option :

Chimie Moléculaire

Intitulée:

**Étude par la chimie informatique, des corrélations structures-
activités/propriétés dans des hétérocycles à intérêt
thérapeutique**

Soutenue le :

Devant la commission d'Examen :

M. OMARI Mahmoud	Professeur	Univ. Biskra	Président
M. BELAIDI Salah	Professeur	Univ. Biskra	Directeur de thèse
M. BOUCEKKINE Abdou	Professeur	Univ. Rennes 1	Co-directeur de thèse
M. BARKAT Djamel	Professeur	Univ. Biskra	Examineur
M. HALET Jean-François	Professeur	Univ. Rennes 1	Invité

Remerciements

La première partie de ce travail a été réalisé au sein de l'équipe de chimie informatique et pharmaceutique du laboratoire de chimie moléculaire et environnement (LMCE) domicilié à l'université Med Khider Biskra.

Je tiens à remercier en premier lieu mon directeur de thèse Mr Salah BELAIDI, Chef de l'équipe de chimie informatique et pharmaceutique et Professeur au Département des Sciences de la Matière, Faculté des Sciences exactes et Sciences de la nature et de la vie, Université Mohamed Khider de Biskra. Un très grand merci pour sa patience sa disponibilité et sa très grande qualité critique vis a vis de mon travail.

La deuxième partie a été préparée à l'unité de recherche U.M.R. 6226 ; Institut des Sciences Chimiques de Rennes (I.S.C.R.), université de Rennes 1, sous la direction du M. Abdou Boucekkine.

Donc, je tiens à remercier mon co-directeur de thèse Abdou Boucekkine, professeur à l'université de Rennes 1. J'ai beaucoup apprécié sa rigueur scientifique et ses critiques constructives, ainsi que ses encouragements qui m'ont permis de gagner en confiance ; sa rigueur et son esprit de synthèse, m'ont considérablement aidé à finaliser une partie ce travail. Je lui exprime mon entière reconnaissance et mon profond respect.

J'exprime ma profonde et respectueuse gratitude à Monsieur Mahmoud OMARI, Chef de département des sciences de la matière et Professeur à l'Université de Biskra, qui m'a fait l'honneur d'accepter de présider le jury de cette thèse.

Je tiens à adresser mes vifs remerciements et à exprimer ma profonde gratitude aux membres de jury : à Mr Jean-François HALET, Directeur de Recherche CNRS à l'Université de Rennes1 et à Mr Djamel BARKAT, Professeur à l'Université de Biskra.

Enfin, j'adresse mes remerciements à tous mes collègues de l'équipe de «chimie informatique et pharmaceutique» du laboratoire de recherche LMCE, université de Biskra et mes collègues du groupe de chimie théorique inorganique à l'unité de recherche U.M.R. 6226 ; Institut des Sciences Chimiques de Rennes (I.S.C.R.), université de Rennes 1.

Une pensée particulière va à l'égard de tous les membres de ma famille qui m'ont soutenue sans relâche durant toutes les années de mes études et qui ont cru en moi, particulièrement ma chère mère, mon cher père, mes frères et mes sœurs.

Contents

CONTENTS.....	4...
GENERAL INTRODUCTION	8...

CHAPITRE I: Theory and Applications of Computational Chemistry

INTRODUCTION.....	13...
QUANTUM METHODS.....	15...
<i>Schrödinger equation</i>	15...
<i>Born-Oppenheimer Approximations</i>	16...
HARTREE-FOCK SELF-CONSISTENT FIELD METHOD.....	17...
<i>Post-HF Methods</i>	17...
<i>Moller-Plesset perturbation theory (MP)</i>	18...
<i>Density-Functional Theory (DFT)</i>	18...
SEMI-EMPIRICAL METHODS.....	20...
MOLECULAR MECHANICS.....	22...

<i>Steric Energy</i>	23...
<i>Examples of MM force fields</i>	25...
METHODS OF GLOBAL MINIMUM.....	28...
The Steepest Descent Method.....	28...
<i>Conjugate Gradient Method</i>	29...
<i>The Newton-Raphson Methods</i>	30...
TYPES OF CALCULATIONS.....	30...
<i>Molecular Geometry</i>	31...
<i>Single Point Calculations</i>	32...
<i>Transition State Calculations</i>	32...
<i>Electronic Density and Spin Calculations</i>	33...
REFERENCES.....	34...

CHAPITRE II: Computational Methods Applied in Physical-Chemistry

property/activity Relationships of Thiophene Derivatives

1. INTRODUCTION.....	38...
2. MATERIALS AND METHODS.....	43...
3. RESULTS AND DISCUSSION.....	44...
3.1. Electronic Structure of thiophene and thiophene systems.....	44...

3.1.1. Electronic structure of thiophene.....	44...
3.1.2. Electronic Structure of substituted thiophenes.....	48...
3.2. Study of structure and physical-chemistry activity relationship for thiophene derivatives.....	57...
3.2. 1. Structural comparison of thiophene derivatives.....	58...
3.2. 2. Structure and physical-chemistry activity relationship.....	61...
3.2. 3. Drug-like calculation on the basis of Lipinski rule of five.....	66...
4. CONCLUSIONS.....	69...
5. REFERENCES.....	71...

CHAPITRE III: Predictive Qualitative Structure-Property / Activity Relationships for Drug Design in some of Antimycobacterial Pyrrole derivatives

1. INTRODUCTION.....	83...
2. MATERIALS AND METHODS.....	87...
3. RESULTS AND DISCUSSION.....	88...
3.1. Geometric and Electronic Structure of pyrrole.....	88...
3.2. Electronic Structure of substituted pyrroles.....	92...
3.3. Study of Structure-Property/ Activity Relationships (SPR/SAR) for Pyrrole Derivatives.....	99...
3.3. 1. Structural comparison of pyrrole derivatives.....	102...
3.3. 2. Structure and physical-chemistry activity relationship.....	104...
3.3. 3. Drug likeness calculation on the basis of Lipinski rule of five.....	108...

4. CONCLUSIONS.....	111...
5. REFERENCES.....	112...

***CHAPITRE IV: Vibronic Coupling to Simulate the Phosphorescence Spectra of
Ir(III) Based OLED Systems: TD-DFT Results Meet Experimental Data***

1. Introduction.....	124
2. Computational details.....	126
3. Results and discussion.....	127
4. 3.1. Ground state geometric structures.....	127
3.2. Ground state electronic structures and electronic vertical excitations..	128
3.3. Luminescence properties.....	132
5. Conclusion.....	135
6. References.....	135
GENERAL CONCLUSION	145
ANNEXES (Publications).....	148

General Introduction

Recently, computational approaches have been considerably appreciated in drug discovery and development. Their applications span almost all stages in the discovery and development pipeline, from target identification to lead discovery, from lead optimization to preclinical or clinical trials. In conjunction with medicinal chemistry, molecular and cell biology, and biophysical methods as well, computational approaches will continuously play important roles in drug discovery. Several new technologies and strategies of computational drug discovery associated with target identification, new chemical entity discovery.

For those engaged in drug design, such as medicinal and computational chemists, the research phase can be broken down into two main tasks: identification of new compounds showing some activity against a target biological receptor, and the progressive optimization of these leads to yield a compound with improved potency and physicochemical properties in silico, in-vitro, and, eventually, improved efficacy, pharmacokinetic, and toxicological profiles in-vivo. Identification of a good lead is a critical first step in drug discovery. The qualities of the lead set the stage for subsequent

efforts to improve therapeutic efficacy through potency against its target, selectivity against related targets, adequate pharmacokinetics, and minimizing toxicity and side effects. Correspondingly, there has been considerable effort to improve technologies in lead discovery. Identification of leads is driven either by random screening or a directed design approach, and traditionally both strategies have been of equal importance, depending on the problem in hand. The directed approach needs a rational starting point for medicinal chemists and molecular modeling scientist to exploit. Examples include the design of analogs of a drug known to be active against a target receptor and mimics of the natural substrate of an enzyme. Increasingly, the three-dimensional structure of many biological targets is being revealed by X-ray crystallography and nuclear magnetic resonance (NMR) spectroscopy, opening the way to the design of novel molecules that directly exploit the structural characteristics of the receptor binding site.

In recent years, this approach of structure-based design has had a major impact on the rational design and optimization of new lead compounds in those cases where the receptor structure is well characterized [1–3]. The practice of testing of large number of molecules for the activity in the model system that is representative of the human

disease, known as screening, is a well-established fact in the pharmaceutical industry. High throughput screening technology allows for the testing of thousands to million of the molecules for activity against a new target system as a part of new drug discovery process [4–5].

Virtual screening, sometime also called in-silico screening, is a new branch of medicinal chemistry that represents a fast and cost effective tool for computationally screening database in search for the novel drug leads. The routes for the virtual screening go back to the structure-based drug design and molecular modeling [6].

Quantum chemistry methods play an important role in obtaining molecular geometries and predicting various properties [7]. To obtain highly accurate geometries and physical properties for molecules that are built from electronegative elements, expensive ab initio/MP2 electron correlation methods are required [8]. Density functional theory methods offer an alternative use of inexpensive computational methods which could handle relatively large molecules.[9-16] Hetero-aromatic ring system is the pivotal part of any biologically active drug molecule. Hetero-aromatic rings are essential because they provide similarity with respect to the biologically active

compounds within our body for e.g. all the nucleic acids, hormones, neurotransmitters etc. which constitutes one or the other hetero-aromatic ring [17].

Druglikeness is a qualitative concept used in drug design, which is estimated from the molecular structure before the substance is even synthesized and tested. The calculation of drug-like property can give us better assumption of biological activity of certain molecules. The theoretical calculation and maintain of certain properties of a molecule can fulfill the parameters which are essential to show certain biological activity. Lipinski's rule of five is a rule of thumb to evaluate druglikeness or determine a chemical compound with a certain pharmacological or biological activity that would make it a likely orally active drug in humans. [18] Drug-likeness appears as a promising paradigm to encode the balance among the molecular properties of a compound that influences its pharmacodynamics and pharmacokinetics and ultimately optimizes their absorption, distribution, metabolism and excretion (ADME) in human body like a drug. [19, 20] Molecular physicochemical and the drug-likeness are the two most significant properties to be considered for a compound to become a successful drug candidate. It is also important for drug development where a pharmacologically active lead structure is

optimized step-wise for increased activity and selectivity, as well as drug-like properties as described by Lipinski's rule [21].

The QSAR is a knowledge-based method where a statistical prediction model is made about biological activity and the presence of molecular descriptors. The aim of carrying out a QSAR study is with the help of computational methods the QSAR model can help evaluate biological activity; this is mostly done to reduce failure rate in the drug development process [22]. The historical aim of QSAR studies is to predict the specific biological activity of a series of test compounds. Nowadays the main objective of these studies is to predict biological activity of In-silico-designed compounds on the basis of already synthesized compounds [23]. The molecular modeling and QSAR calculations are used in many fields specially, physics, chemistry, biology, material science as well as tissue engineering and drug design.[24-27]

Multiple linear regression (MLR), which is one of the most common and simplest method for constructing QSAR models, was used in this study [28–30]. The advantage of MLR is that it is simple to use and the derived models are easy to interpret.

- ❖ Our work is placed in the context of fundamental and original research of some heterocyclic compound and their derivatives, the main objective of this work is the application of different methods of molecular modeling to predict the chemical reactivity, physical property and biological activity expected in new molecules.

The structure of the memory, composed by four chapters, has been conceptually divided into two differentiated parts. On one hand, the bibliographic background section, which is composed by chapter 1. On the other hand, chapter 2, chapter 3 and chapter 4 devoted to applications and results, deepens into specific practical applications. The content of the chapters is briefly described:

- ❖ **Chapter 1 : Theory and Applications of Computational Chemistry**

This chapter contains the main concepts and definitions related to computational methods (quantum mechanics methods, Semi-empirical methods and molecular mechanics methods).

- ❖ **Chapter 2 : *Computational Methods Applied in Physical-Chemistry property***

Relationships of Thiophene Derivatives

The second chapter contains a structural, electronic and energetic study of Thiophene and its derivatives. In this chapter, we present the results of a comparative study on two methods used in the calculation of the density functional theory (DFT) and ab initio, as well, the substitution effect on energy and electronic parameters of the basic nucleus of Thiophene /work published in: Journal of Computational and Theoretical Nanoscience, Vol. 12, 1737–1745, 2015.

❖ **Chapter 3 : *Predictive Qualitative Structure-Property / Activity Relationships***

for Drug Design in some of Antimycobacterial Pyrrole derivatives

This chapter highlights the importance of a qualitative study of structure-property/ Activity relationships and drug likeness proprieties of a bioactive series Pyrrole derivatives (work published in: Quantum Matter, Vol. 5, 1–8, 2016)

❖ **Chapter 4 : *Vibronic Coupling to Simulate the Phosphorescence***

Spectra of Ir(III) Based OLED Systems: TD-DFT Results Meet

Experimental Data

In this chapter we investigate theoretically the electronic and optical properties of six based Iridium imidazolylidene complexes serving as serious candidates for OLED systems. Computations using methods rooted into DFT and TD-DFT explain the observed optical properties. Observed absorption bands have been assigned and computations of the lowest triplet excited states have been performed. The use of vibronic coupling permitted to reproduce and explain the structured phosphorescence spectrum of complexes.

- [1] Greer J., Erickson J.W., Baldwin J.J., Varney M.D. Application of the three-dimensional structures of protein target molecules in structure-based drug design. *J. Med. Chem.* 1994; 37:1035–1054.
- [2] Bohacek R.S., McMartin C., Guida W.C. The art and practice of structure-based drug design: A molecular modeling perspective. *Med. Res. Rev.* 1996; 16: 3–50.
- [3] Shoichet B.K., Bussiere D.E. The Role of Macromolecular Crystallography and Structure for Drug Discovery: Advances and Caveats. *Curr. Opin. Drug Discov. Dev.* 2000; 3: 408–422.

- [4] Wodak S.J., Janin J. , Computer analysis of protein-protein interaction. *J. Mol. Biol.*1978; 124:323–342.
- [5] Kuntz I.D., Blany J.M., Oatley S.J., Langridge R, Ferrin T.E. A geometric approach to macromolecule-ligand interactions. *J. Mol. Biol.*1982; 161: 269–288.
- [6] Mugge I., Enyedy I. Virtual Screening. Medicinal chemistry and Drug discovery. 6 th ed Volume 1; Verginia : Wiley Interscience , 2003: 243–279.
- [7] M. Ciobanu, L. Preda, D. Savastru, R. Savastru, and E. M. Carstea, *Quantum Matter* 2, 60,(2013)
- [8]A. Srivastava, N. Jain, and A. K. Nagawat, *Quantum Matter* 2, 307-313 (2013)
- [9] M. Narayanan and A. J. Peter, *Quantum Matter*, 1, 53, (2012)
- [10]Gregorio H. Coccoletzi and Noboru Takeuchi, *Quantum Matter* 2, 382-387 (2013)
- [11]Medhat I. and H. Elhaes, *Rev. Theor. Sci.* 1, 368-376 (2013)
- [12]E. C. Anota, H. H. Coccoletzi, and M. Castro, *J. Comput. Theor. Nanosci.* 10, 2542-2546 (2013)
- [13]F. Bazooyar, M. Taherzadeh, C. Niklasson, and K. Bolton, *J. Comput. Theor. Nanosci.* 10, 2639-2646 (2013)

- [14] H. Langueur, K. Kassali, and N. Lebgaa, *J. Comput. Theor. Nanosci.*, 10, 86, **(2013)**
- [15] S. Belaidi, H. Belaidi and D. Bouzidi, *J. Comput. Theor. Nanosci.* 12, 1737–1745, 2015
- [16] M. Narayanan and A. John Peter, *Quantum Matter. 1*, 53 **(2012)**
- [17] R. O. Bora, B. Dar, V. Pradhan and M. Farooqui, *Mini. Rev. Med. Chem.* 13, 7, **(2013)**
- [18] J. Mazumder, R. Chakraborty, S. Sen, S. Vadra, B. De and T. K. Ravi, *Der. Pharma. Chemica.* 1(2), 188-198 (2009)
- [19] C. A. Lipinski, F. Lombardo, B. W. Dominy, and P. J. Feeney, *Adv. Drug Deliv. Rev.* 64, 4 **(2012)**.
- [20] G. Vistoli, A. Pedretti, and B. Testa, *Drug. Discov. Today* 13, 285 **(2008)**.
- [21] C. A. Lipinski, F. Lombardo, B.W.Dominy, P. J. Feeney. *Adv Drug Deliv Rev.* 46, 03-26.**(2001)**

- [22] C.Y. Liew, C.W. Yap, In: Current Modeling Methods Used in QSAR/QSPR. Statistical Modeling of Molecular Descriptors in QSAR/QSPR; Eds.; Wiley-Blackwell: Weinheim, 2012, 1st ed,1-32.
- [23] T. D. C. Mark, In: Quantitative Structure-Activity Relationships (QSARs)- Applications and Methodology; Eds.; Springer Dordrecht Heidelberg: New York, 2010,8, 16-24.
- [24]. Y. Belmiloud, M. Ouraghi, M. Brahimi, A. Benaboura, D. Charqaoui, and B. Tangour, *J. Comput. Theor. Nanosci.*9, 1101 (2012).
- [25]. M. Ibrahim, N. A. Saleh, J. H. Ali, W. M. Elshemey, and A. A. Elsayed, *J. Spectrochim. Acta, Part A: Molecular and Biomolecular Spectroscopy*75, 702(2010).
- [26]. M. Ibrahim, *J. Comput. Theor. Nanosci.*6, 682(2009).
- [27]. M. E. El-Sayed, O. Amina, M. Ibrahim, and I. A. Wafa, *J. Comput. Theor. Nanosci.*6, 1669 (2009).
- [28] S. Clementi, S.Wold, How to choose the proper statistical method, in: H.V.D. Waterbeemd (Ed.), Chemometrics Methods in Molecular Design, VCH, Weinheim, 1995, pp. 319–338.

[29] P.D. Berger, R.E. Maurer, *Experimental Design with Applications in Management, Engineering and Sciences*, 2002 (Duxbury, USA).

[30] C.W. Yap, Y. Xue, H. Li, Z.R. Li, C.Y. Ung, L.Y. Han, C.J. Zheng, Z.W. Cao, Y.Z. Chen, *Mini. Rev. Med. Chem.* 6 (4), 449–459 (2006).

CHAPITRE I:**Theory and Applications of
Computational Chemistry**

INTRODUCTION

Chemists have been doing computations for centuries, but the field we know today as “computational chemistry” is a product of the digital age. Martin Karplus, Michael Levitt, and Arieh Warshel won the 2013 Nobel Prize in Chemistry for work that they did in the 1970s, laying the foundations for today's computer models that combine principles of classical (Newtonian) physics and quantum physics to better replicate the fine details of chemical processes. In 1995, three computational chemists, Paul Crutzen, Mario Molina, and F. Sherwood Rowland, won the Chemistry Nobel for constructing mathematical models that used thermodynamic and chemical laws to explain how ozone forms and decomposes in the atmosphere. However, computational chemistry was not generally thought of as its own distinct field of study until 1998, when Walter Kohn and John Pople won the Chemistry Nobel for their work on density functional theory and computational methods in quantum chemistry. Computational chemistry is not the same as computer science, although professionals in the two fields commonly collaborate. Computer scientists devote their time to developing and validating computer algorithms,

software and hardware products, and data visualization capabilities. Computational chemists work with laboratory and theoretical scientists to apply these capabilities to modeling and simulation, data analysis, and visualization to support their research efforts.

Many computational chemists develop and apply computer codes and algorithms, although practicing computational chemists can have rewarding careers without working on code development. Programming skills include compiling FORTRAN or C code, performing shell scripting with bash, Tcl/Tk, python, or perl, performing statistical analysis using R or SPSS, and working within a Windows, MacOS, or Linux environment.

As cheminformatics tools and computational modeling platforms develop, it becomes easier to define workflow tasks through graphically based workbench environments. A recent trend in reduced-order modeling and similar methods is enabling fairly powerful computational tools to be implemented on portable devices, including tablets and smart phones. This enables researchers to perform what-if calculations and try out various scenarios while they are in the plant or out in the field. [1]

Molecular modeling can be considered as a range of computerized techniques based on Computational chemistry methods and experimental data that can be used either to analyze molecules and molecular systems or to predict molecular, chemical, and biochemical properties[2-4]. It serves as a bridge between theory and experiment to:

1. Extract results for a particular model.
2. Compare experimental results of the system.
3. Compare theoretical predictions for the model.
4. Help understanding and interpreting experimental observations.
5. Correlate between microscopic details at atomic and molecular level and macroscopic properties.
6. Provide information not available from real experiments.

All molecular calculation techniques can be classified under three general categories:

- ❖ ab initio and density functional electronic structure calculations,
- ❖ semi-empirical methods,
- ❖ empirical methods and Molecular Mechanics

QUANTUM METHODS

Schrödinger equation

The starting point of the following overview is the Schrödinger equation[5 - 8] in its time dependent and time independent forms (1) and (2) respectively

$$\frac{\partial \Psi}{\partial t} = -\frac{i}{\hbar} \hat{H} \Psi \quad (1)$$

$$\hat{H} \Psi = E \Psi \quad (2)$$

where the wave functions Ψ and Ψ are functions of all coordinates of the relevant system and Ψ is also a function of time. In our case of a molecular Hamiltonian \hat{H} is given by:

$$\hat{H} = -\frac{\hbar^2}{2} \sum_I \frac{1}{m_I} \nabla_I^2 - \frac{\hbar^2}{2m_e} \nabla_i^2 + \sum_I \sum_{J < I} \frac{Z_I Z_J e^2}{r_{IJ}} - \sum_I \sum_i \frac{Z_I e^2}{r_{iI}} + \sum_j \sum_{i > j} \frac{e^2}{r_{ij}} \quad (3)$$

where I and J refer to the nuclei i and j refer to electrons. The first term in (3) is the operator of the kinetic energy of the nuclei. The second term is the operator of the kinetic energy of the electrons. The third term is the potential energy of repulsions

between the nuclei, r_{IJ} is the distance between the nuclei I and J with atomic numbers Z_I and Z_J . The fourth term is the potential energy of the attractions between the electrons and the nuclei and r_{iI} is the distance between electron i and nucleus I. The last term is the potential energy of the repulsions between the electrons, r_{ij} is the distance between electrons i and j .

Born-Oppenheimer Approximations:

simplifies the general molecular problem by separating nuclear and electronic motions. This approximation is reasonable since the mass of a typical nucleus is thousands of times greater than that of an electron. The nuclei move really slowly with respect to the electrons. Thus, the electronic motion can be described as occurring in a field of fixed nuclei.

We can use the Born-Oppenheimer approximation to construct an electronic Hamiltonian, which neglects the kinetic energy term of the nuclei,

$$\hat{H} = -\frac{\hbar^2}{2m_e} \nabla_i^2 + \sum_I \sum_{J < I} \frac{Z_I Z_J e^2}{r_{IJ}} - \sum_I \sum_i \frac{Z_I e^2}{r_{iI}} + \sum_j \sum_{i > j} \frac{e^2}{r_{ij}} \quad (4)$$

This Hamiltonian is used in the Schrödinger equation describing the motion of the electrons in the field of the fixed nuclei:

$$\hat{H}^{elec} \Psi^{elec} = E^{eff} \Psi^{elec} \quad (5)$$

Solving this equation for the electronic wave function will produce the effective-nuclear potential function E^{eff} that depends on the nuclear coordinates and describes the potential energy surface of the system. For bond electronic problem, Ψ should satisfy two requirements: antisymmetry and normalization. Ψ should change sign when two electrons of the molecule interchange and the integral of Ψ over all space should be equal to the number of electrons of the molecule.

HARTREE-FOCK SELF-CONSISTENT FIELD METHOD

Much of the difficulty of solving the Schrödinger equation stems from the need to simultaneously determine the energy of each electron in the presence of all other electrons.

In the Hartree-Fock (HF) method this is avoided by calculating the energy of each

electron in the averaged static field of the others. Initially a guess is made of the electron energies.

The energy of each electron is then calculated in the field of the initial electron configuration. This procedure is repeated in an iterative loop until convergence (Self-Consistent referring to this iterative calculation).

The Hartree-Fock method can therefore be thought of as a kind of mean-spherical approximation at the electron level. The difference between the Hartree-Fock energy and the energy for the full Schrödinger equation is called the correlation energy.

Hartree-Fock calculations are sufficiently accurate to provide insight into many problems and they are widely used. As Hartree-Fock calculations have been applied to different problems it has however become increasingly clear that the correlation energy is of great significance in determining the properties of a system. Efforts have therefore been made to improve on the Hartree-Fock energy.

Post-HF Methods

There are a number of different methods that go beyond Hartree-Fock calculations, one of the widely used approaches is perturbation theory. In perturbation theory the Hartree-Fock solution is treated as the first term in a Taylor series. The perturbation terms added involve the electron repulsion. One of the more common forms was developed by Møller and Plesset. The second order perturbation form is referred to as MP2. This form will be utilized in the present work.

It should be noted that the electron-electron repulsion energy is not necessarily a small perturbation. In cases in which this term is large the application of perturbation theory can become more difficult.

There are a number of other techniques to include electron correlation that can potentially provide very accurate results, such calculations can however become very time consuming and at present they tend to be used for small molecules with maybe 3-4 heavy (non-hydrogen) atoms. The molecules studied in the present work are somewhat larger and the decision has been made not to use such time-consuming methods.

Moller-Plesset perturbation theory (MP)

The Moller-Plesset (MP) Perturbation Theory attempts to correct the HF theory, which as mentioned earlier provides an approximation for the repulsion term between electrons and determines the position of an electron solely with respect to the atom's nucleus and the average of other electrons. As this model is not quite accurate, the MP theory uses HF as a starting point and then corrects it for the attraction term between the nucleus and the electron as well as the position of an electron with respect to another electron. The number following MP, such as MP2 or MP3, indicates the number of perturbations, or approximation terms, used in the theory. Generally, the higher this number, the greater the accuracy of the method.

Density-Functional Theory (DFT)

DFT theory models electron correlation as a functional of the electron density, ρ . The functional employed by current DFT methods partitions the electronic energy via the Kohn-Sham equations [9, 10] into several terms :

$$E = E^T + E^V + E^J + E^{XC} \quad (6)$$

where E^T is the kinetic energy term (arising from the motion of the electrons), E^V is the potential energy term that includes nuclear-electron and nuclear-nuclear interactions, E^J is the electron-electron repulsion term and E^{XC} is the electron correlation term. All terms except nuclear-nuclear repulsions are functions of the electron density. The terms $E^T + E^V + E^J$ represent the classical energy of the electron distribution, while E^{XC} represents both the quantum mechanical exchange energy, which accounts for electron spin, and the dynamic correlation energy due to the concerted motion of individual electrons.

Pure DFT methods calculate E^{XC} by pairing an exchange functional with a correlation functional and so are designated by the choice of combination. For example, BLYP combines Becke's gradient-corrected exchange functional with the gradient-corrected correlation functional of Lee, Yang and Parr [11].

DFT calculations fall into three general categories: local density approximations (LDA), generalised gradient approximations (GGA), and "hybrid" combinations of DFT and

Hartree-Fock terms. LDA exchange and correlation functionals only contain terms related to electron density- an approach that works for some bulk materials, but fails to accurately predict properties in isolated molecules. GGA ("nonlocal") functionals contain terms that depend upon both the electron density and the density gradients. The gradient-corrected density functional method BLYP is capable of predicting intramolecular bond dissociation energies to within a few kJ/mol [12]. However, the generalised gradient approximation severely underestimates activation barriers for some reactions due to neglect of Coulomb "self-interaction" of the electrons [13]. This problem is remedied with hybrid methods that combine Hartree-Fock self-interaction corrections with density functional exchange and correlation. Examples of hybrid methods are B3LYP and B3PW91, where B3 denotes Becke's three-parameter hybrid functional [14,15], while 'PW91' and 'LYP' are gradient-corrected correlation functionals of Perdew and Wang [16] and, as above, Lee, Yang and Parr.

SEMI-EMPIRICAL METHODS

Most molecular computations done by organic chemists, especially those examining minimum energy geometries, are done using this method because it provides the best

compromise between speed and accuracy. This method can be thought of as a hybrid of molecular mechanics-type models based on experimentally measured empirical data and pure theory quantum chemical, thus the name semi-empirical. It uses the Schrödinger equation approximations, but in order to make the calculations less time-consuming, it only calculates the locations of valence electrons, not all electrons. For the inner shell electrons, empirical data from typical organic molecules is used to estimate their locations.

These semiempirical methods are presented by :

❖ **MNDO method (Modified Neglect of Diatomic Overlap)**[17] which takes in account the repellencies between the electrons pairs and the electron-electron perellence directions;

❖ **ZDO method (zero differential overlap)** is based on the Huckel method for the π electrons

❖ **CNDO method (Complete Neglect of Differential Overlap)** which takes in account only the atomic orbital of spherical symmetry and assesses therepellece integrals as the orbital would be sphere. In this case are two methodsCNDO/1 and CNDO/2 which are used for the spectrum parameters;

❖ **INDO method**[18](Intermediate Neglect of Differential Overlap) which includes the monoelectronic repellece integrals between atomic orbital of the same atom;

❖ **NDDO method (Neglect of Differential diatomic orvelap)**which takes in account the orientation direction of the orbital; MINDO/3[19] method is an particular case of the NNDO method which assesses the monoelectronic repellece integrals;

❖ **SAM1 (Semi-Ab-Initio Model 1)**

The final 1993 offering in Michael Dewar's name was Semi-Ab-Initio Model 1 [20].

In SAM1, two-electron integrals are calculated using a standard STO-3G basis set (and hence the appearance of ab initio in the title). The resulting integrals were then scaled,

and the Gaussian terms in the core–core repulsions were retained in order to fine-tune the calculations.

❖ **AM1 (Austin Model 1)**

Next came Austin model 1 (AM1), due to M. J. S. Dewar et al. [21]. AM1 was designed to eliminate the problems from MNDO caused by a tendency to overestimate repulsions between atoms separated by the sum of their van der Waals radii. The strategy adopted was to modify the core–core terms by multiplication of the Coulomb term with sums of Gaussian functions. In the original AM1 paper there are four terms in the Gaussian expansion. Each Gaussian is characterized by its position along the A–B vector and by its width. This significantly increased the number of parameters for each atom.

The performances of the semiempirical method consist in the smaller cost of them and in their speed, but also in the fact they can determine some properties that can not be established experimentally.

❖ **PM3 (parameterized method 3)**

PM3 is the third parameterization of MNDO, and the PM3 model contains essentially all the same terms as AM1. The parameters for PM3 were derived by J. J. P. Stewart [22]

in a more systematic way than for AM1, many of which were derived by ‘chemical intuition’. As a consequence, some of the parameters are quite different from those of MNDO but the two models seem to predict physical properties to the same degree of accuracy.

MOLECULAR MECHANICS

Molecular mechanics (MM) describes molecules in terms of “bonded atoms”, which have been distorted from some idealized geometry due to non-bonded van der Waals and Coulombic interactions. [23, 24]

Molecular mechanics calculates the energy of a molecule and then adjusts the energy through changes in bond lengths and angles to obtain the minimum energy structure.

Molecular mechanics models are useful in studying structures, conformational energies and other molecular properties, including vibrational frequencies, conformational entropies and dipole moments, etc. [25, 44].

Steric Energy

A molecule can possess different kinds of energy such as bond and thermal energy.

Molecular mechanics calculates the steric energy of a molecule (the energy due to the geometry or conformation of a molecule). Energy is minimized in nature, and the conformation of a molecule that is favored is the lowest energy conformation.

Knowledge of the conformation of a molecule is important because the structure of a molecule often has a great effect on its reactivity. The effect of structure on reactivity is important for large molecules like proteins. Studies of the conformation of proteins are difficult and therefore interesting, because their size makes many different conformations possible.

Molecular mechanics assumes the steric energy of a molecule to arise from a few, specific interactions within a molecule. These interactions include the stretching or compressing of bonds beyond their equilibrium lengths and angles, torsional effects of twisting about single bonds, the Van der Waals attractions or repulsions of atoms that come close together, and the electrostatic interactions between partial charges in a molecule due to polar bonds. To quantify the contribution of each, these interactions can

be modeled by a potential function that gives the energy of the interaction as a function of distance, angle, or charge[23,29].

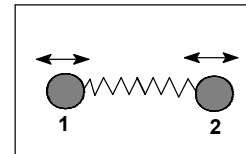
The total steric energy of a molecule can be written as a sum of the energies of the interaction:

$$E_{steric\ energy} = E_{stret} + E_{bend} + E_{tor} + E_{VDW} + E_{qq} + \dots \quad (7)$$

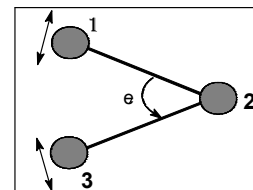
The bond stretching, bending and torsion interactions are called bonded interactions because the atoms involved must be directly bonded or bonded to a common atom. The Van der Waals and electrostatic (qq) interactions are between non-bonded atoms.

$$\begin{aligned} E_{steric\ energy} &= E_{tot} \\ &= \sum_{bonds} k_r (r - r_{eq})^2 + \sum_{bonds} k_\vartheta (\vartheta - \vartheta_{eq})^2 + \sum_{bonds} \frac{V_n}{2} [1 + \cos(n\Phi - \gamma)] \\ &\quad + \sum_{i < j} \frac{A_{ij}}{R_{ij}^{12}} - \frac{B_{ij}}{R_{ij}^6} + \sum_{i < j} \frac{q_i q_j}{\epsilon R_{ij}} \quad (8) \end{aligned}$$

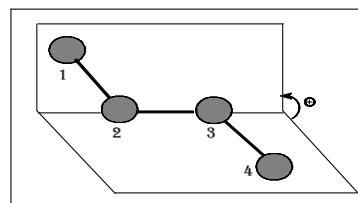
$$E_{str} = \sum_{bonds} k_r (r - r_{eq})^2 \quad (9)$$



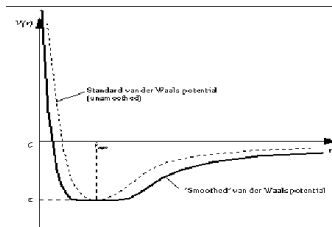
$$E_{bend} = \sum_{bonds} k_\vartheta (\vartheta - \vartheta_{eq})^2 \quad (10)$$



$$E_{tor} = \sum_{bonds} \frac{V_n}{2} [1 + \cos(n\Phi - \gamma)] \quad (11)$$



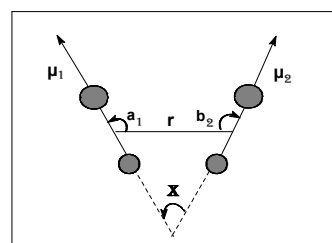
$$E_{vdw} = \sum_{i < j} \frac{A_{ij}}{R_{ij}^{12}} - \frac{B_{ij}}{R_{ij}^6} \quad (12)$$



$$E_{qq} = \sum_{i < j} \frac{q_i q_j}{\epsilon R_{ij}} \quad (13)$$

and

$$E(e) = \mu_1 \mu_2 (\cos X - 3 \cos a_1 \cdot \cos b_2) / D \cdot r_{12}^3 \quad (14)$$



Examples of MM force fields :

In Common use are:

✓ **AMBER**

(Assisted Model Building with Energy Refinement) - primarily designed for the study of biomolecules such as proteins and nucleotides [45].

✓ **CHARMM**

(Chemistry at HARvard Molecular Mechanics) - primarily designed for biological and pharmaceutical study, but has also been applied to micelles and self-assembling macromolecules [46].

✓ **MM_x** (MM2, MM3, etc)

Optimised for structural and thermodynamic studies of small non-polar molecules [47].

MM_x force fields include third- and fourth-order corrections to standard quadratic fits for the potential energy surfaces of bonds and bond angles, thus allowing for non-harmonic effects in molecular vibrations. The various MM_x versions differ primarily in their parameterisations. The higher versions tend to be more modern and address deficiencies in their predecessors. However, for the newer versions such as MM4, parameters may not be available for all classes of molecules.

✓ **OPLS**

(Optimised Potentials for Liquid Simulations)-optimised for reproducing the physical properties of biomolecules in liquid solutions [47].

The authors are not aware of any published study discussing the use of AMBER, CHARMM, MMx or OPLS with energetic materials. Since these packages are optimised for biochemistry and pharmaceutical applications, it is unlikely that they will accurately reproduce the behaviour of energetic materials without further modification. However, it is likely they can be used for limited applications with only slight modification.

✓ **CFF**

The consistent force field (CFF) [48-51] was developed to yield consistent accuracy of results for conformations, vibrational spectra, strain energy, and vibrational enthalpy of proteins. There are several variations on this, such as the Ure-Bradley version (UBCFF), a valence version (CVFF), and Lynghy CFF. The quantum mechanically parameterized force field (QMFF) was parameterized From ab initio results. CFF93 is a rescaling of QMFF to reproduce experimental results. These force fields use five to six valence terms, one of which is an electrostatic term, and four to six cross terms.

✓ **DREIDING[52]**

DREIDING is an all-purpose organic or bio-organic molecule force field. It has been most widely used for large biomolecular systems. It uses five valence terms, one of which is an electrostatic term. The use of DREIDING has been dwindling with the introduction of improved methods.

✓ **MMFF**

The Merck molecular force field (MMFF) is one of the more recently published force fields in the literature. It is a general-purpose method, particularly popular for organic molecules. MMFF94[53] was originally intended for molecular dynamics simulations, but has also seen much use for geometry optimization. It uses five valence terms, one of which is an electrostatic term, and one cross term.

✓ **MOMECC**

MOMECC[54] is a force field for describing transition metal coordination compounds. It was originally parameterized to use four valence terms, but not an electrostatic term. The metal-ligand interactions consist of a bond-stretch term only. The coordination

sphere is maintained by nonbond interactions between ligands. MOMEC generally works reasonably well for octahedrally coordinated compounds.

✓ **GROMOS**

(Groningen Molecular Simulation) developed at the University of Groningen and the ETH (Eidgenössische Technische Hochschule) of Zurich [55] is quite popular for predicting the dynamical motion of molecules and bulk liquids, also being used for modelling biomolecules. It uses five valence terms, one of which is electrostatic [56]. Its parameters are currently being updated [57].

Energy Minimization and Geometry Optimization

The basic task in the computational portion of MM is to minimize the strain energy of the molecule by altering the atomic positions to optimal geometry. This means minimizing the total nonlinear strain energy represented by the force field equation with respect to the independent variables, which are the Cartesian coordinates

of the atoms[58]. The following issues are related to the energy minimization of a molecular structure:

- The most stable configuration of a molecule can be found by minimizing its free energy, G .
- Typically, the energy E is minimized by assuming the entropy effect can be neglected.
- At a minimum of the potential energy surface, the net force on each atom vanishes, therefore the stable configuration.

Because the energy zero is arbitrary, the calculated energy is relative. It is meaningful only to compare energies calculated for different configurations of chemically identical systems.

- It is difficult to determine if a particular minimum is the global minimum, which is the lowest energy point where force is zero and second derivative matrix is positive definite. Local minimum results from the net zero forces and positive definite second derivative matrix, and saddle point results from the net zero forces and at least one negative eigenvalue of the second derivative matrix.

METHODS OF GLOBAL MINIMUM

The most widely used methods fall into two general categories:

(1) steepest descent and related methods such as conjugate gradient, which use first derivatives, and

(2) Newton Raphson procedures, which additionally use second derivatives.

The Steepest Descent Method:

depends on:

Either calculating or estimating the first derivative of the strain energy with respect to each coordinate of each atom and moving the atoms. [59]

The derivative is estimated for each coordinate of each atom by incrementally moving the atom and storing the resultant strain energy change. The atom is then returned to its original position, and the same calculation is repeated for the next atom. After all the atoms have been tested, their positions are all changed by a distance proportional to the derivative calculated in step 1. The entire cycle is then repeated. The calculation is

terminated when the energy is reduced to an acceptable level. The main problem with the steepest descent method is that of determining the appropriate step size for atom movement during the derivative estimation steps and the atom movement steps. The sizes of these increments determine the efficiency of minimization and the quality of the result. An advantage of the first-derivative methods is the relative ease with which the forcefield can be changed.

Conjugate Gradient Method:

Is a first-order minimization technique. It uses both the current gradient and the previous search direction to drive the minimization. Because the conjugated gradient method uses the minimization history to calculate the search direction and contains a scaling factor for determining step size, the method converges faster and makes the step sizes optimal as compared to the steepest descent technique. However, the number of computing cycles required for a conjugated gradient calculation is approximately proportional to the number of atoms (N), and the time per cycle is proportional to N . The Fletcher-Reeves approach chooses a descent direction to lower energy by considering the current gradient, its conjugate, and the gradient for the previous step.

The Polak-Ribiere algorithm improves on the Fletcher-Reeves approach by additional consideration of the previous conjugate and tends to converge more quickly.

The Newton-Raphson Methods

Energy minimization [23] utilize the curvature of the strain energy surface to locate minima. The computations are considerably more complex than the first-derivative methods, but they utilize the available information more fully and therefore converge more quickly. These methods involve setting up a system of simultaneous equations of size $(3N-6)(3N-6)$ and solving for the atomic positions that are the solution of the system. Large matrices must be inverted as part of this approach.

The general strategy is to use steepest descents for the first 10-100 steps (500-1000 steps for proteins or nucleic acids) and then use conjugate gradients or Newton-Raphson to complete minimization for convergence (using RMS gradient or/and energy difference as an indicator). For most calculations, RMS gradient is set to 0.10 (you can use values greater than 0.10 for quick, approximate calculations).

The calculated minimum represents the potential energy closest to the starting structure of a molecule. The energy minimization is often used to generate a structure at a stationary point for a subsequent single-point calculation or to remove excessive strain in a molecule, preparing it for a molecular dynamic simulation.

TYPES OF CALCULATIONS

Computational chemistry (also called molecular modelling; the two terms mean about the same thing) is a set of techniques for investigating chemical problems on a computer. Questions commonly investigated computationally are:

Molecular Geometry:

Molecular geometry is the [three-dimensional](#) arrangement of the [atoms](#) that constitute a [molecule](#). It determines several properties of a substance including its [reactivity](#), [polarity](#), [phase of matter](#), [color](#), [magnetism](#), and [biological activity](#). The angles between bonds that an atom forms depend only weakly on the rest of molecule, i.e. they can be understood as approximately local and hence [transferable properties](#).

The molecular geometry can be determined by various methods and diffraction methods. IR , microwave and Raman spectroscopy can give information about the molecule geometry from the details of the vibrational and rotational absorbance detected by these techniques. X-ray crystallography , neutron diffraction and electron diffraction can give molecular structure for crystalline solids based on the distance between nuclei and concentration of electron density. Gas electron diffraction can be used for small molecules in the gas phase.

NMR and FRET methods can be used to determine complementary information including relative distances, dihedral angles, angles, and connectivity. Molecular geometries are best determined at low temperature because at higher temperatures the molecular structure is averaged over more accessible geometries.

Larger molecules often exist in multiple stable geometries (conformational isomerism) that are close in energy on the potential energy surface . Geometries can also be computed by ab initio quantum chemistry methods to high accuracy. The molecular geometry can be different as a solid, in solution, and as a gas [60].

Geometry Optimization

The standard computational chemistry calculation to find the lowest energy or most relaxed conformation for a molecule. The approach is the same for all levels of calculation, involving an iterative “jiggling” process like that described for molecular mechanics.

At each step, the molecular geometry is modified slightly and the energy of the molecule is compared with the last cycle. The computer moves the molecule a little, calculates the energy, moves it a little more, and keeps going until it finds the lowest energy. This is the energy minimum of the molecule and is obtained at the optimized geometry. Recall that the energies from molecular mechanics can only be used in a relative sense, while those from quantum electronic structure methods can be compared in an absolute sense, like heats of formation.

Single Point Calculations

are often used in combination with a geometry optimization to investigate steric hindrance. In this case the method only performs one computational cycle to calculate

the energy of a particular fixed geometry [3]. In a thermodynamically controlled reaction, the energetic difference between two conformations is often due to steric hindrance. If the product molecule optimizes in one conformation, you can use single point calculations to determine how much more energy is needed to form the non-preferred conformation.

The structure drawing and manipulation part of the software will allow you to move only that part of the molecule that changes in the higher energy form, leaving the rest of the molecule optimized.

The single point calculation performed on this modified molecule will give an energy that you can directly compare with the optimized energy to find the energy difference between the lower and higher energy conformers. For example, the energetic difference between having a constituent in the axial or equatorial position on a cyclohexane ring can be determined.

Transition State Calculations

Can be thought of as the reverse of geometry optimizations. In this case, the method searches for a structure of maximum energy, a transient intermediate which cannot be isolated experimentally. For example, this type of calculation allows one to examine transition state energies and geometries of intermediates involved in carbocation rearrangements[7].

The literature contains standard models that should use as the starting point for these calculations. It takes a far amount of effort and experience to properly analyze transition state structures and energies.

Electronic Density and Spin Calculations,

Allow visualization of electronic properties such as electron densities, electrostatic potentials, spin densities and the shapes and signs of molecular orbitals. The values for a particular property at each point in the 3-dimensional space around a molecule are displayed on the 2-dimensional computer screen as a surface of constant numerical value, often called an isosurface which can be rotated in any direction to study it.

Alternately, numerical variations of a given property (such as electron density) at a defined distance from the molecule can be displayed as property maps using color as a key yielding what is called a property map. Carrying out surface calculations and viewing their graphical representations are major activities in computational chemistry and can provide useful insight into the mechanisms of organic reactions[60].

REFERENCES

- [1] H. Dorsett and A. White, Overview of Molecular Modelling and Ab initioMolecular Orbital Methods Suitable for Use with Energetic Materials, Salisbury South Australia 5108 Australia,9, (2000).
- [2] H.-D. Höltje, and G.Folkeis, Molecular Modeling: Basic Principles and Applications. VCH, New York (1997).
- [3] A.R.Leach, Molecular Modeling Principles and Applications.Longman, Essex (1996).
- [4] M. F.Schlecht, Molecular Modeling on the PC. Wiley-VCH, New York (1998).

- [5] I. N. Levine, Quantum Chemistry, Fifth Edition. New Jersey: Prentice-Hall, Inc (2000).
- [6] D. J. Griffiths, Introduction to Quantum Mechanics. New Jersey: Prentice-Hall, Inc (1995).
- [7] J. B. Foresman and Æ.Frisch. Exploring Chemistry with Electronic Structure Methods, Second Edition. U. S. A: Gaussian, Inc (1993).
- [8] Æ. Frisch, and M. J.Frisch, Gaussian 98 User's Reference, Second Edition. U. S. A.: Gaussian, Inc (1999).
- [9] R.G. Parr, and W.Yang, Density-Functional Theory of Atoms and Molecules, in International Series of Monographs on Chemistry, Breslow, R., Goodenough, J.B., Halpern, J., and Rolinson, J., Eds., Oxford University Press, New York(1989).
- [10] D. Joubert, Ed. Density Functionals: Theory and Applications, Springer-Verlag, Heidelberg, DE (1998).
- [11] C. Lee, W.Yang, and R.G. Parr, *Phys. Rev.b*.37(2) 785-789 (1988).
- [12] W. Kohn, A.D.Becke, and R.G. Parr. *J. Phys. Chem.*100(31) 12974-12980 (1996).

- [13] J.L. Durant, *Chem. Phys. Lett.* 256, 595-602 (1996).
- [14] A.D. Becke, *Phys. Rev. A* 38(6) 3098-3100 (1998).
- [15] A.D. Becke, *J. Chem. Phys.* 98(7) 5648-5652 (1993).
- [16] J.P. Perdew, K. Burke, and Y. Wang, *Phys. Rev. B* 54 (23) 16533-16539 (1996).
- [17] M.J.S. Dewar, G.L. Gladys, J.J. P. Stewart, *J. Am. Chem. Soc.* 106, 6771 (1978).
- [18] W.P. Anderson, T. Cundari, R. Dargatzis, M.C. Zerner, *Inorg. Chem.* 29, 1 (1990).
- [19] D. F. V. Lewis, *Chem. Rev.* 86, 1111 (1986).
- [20] M. J. S. Dewar, C. Jie and J. Yu, *Tetrahedron* 49, 5003 (1993).
- [21] M. J. S. Dewar, E. G. Zoebisch, E. F. Healey and J. J. P. Stewart, *J. Am. Chem. Soc.* 107, 3902 (1985).
- [22] J. J. P. Stewart, *J. Comp. Chem.* 10, 209- 221 (1989).
- [23] U. Burkert and N.L. Allinger, *Molecular Mechanics*, ACS Monograph no. 177, American Chemical Society, Washington D.C., (1982)
- [24] A.K. Rappe and C.J. Casewit, *Molecular Mechanics Across Chemistry*, University Science Books, Sausalito, CA, (1997).

- [25] W.D. Cornell, P. Cieplak, C.I. Bayly, I.R. Gould, K.M. Merz Jr., D.M. Ferguson, D.C. Spellmeyer, T. Fox, J.W. Caldwell, P.A. Kollman, *J. Am. Chem. Soc.* 117, 5179–5197 (1995).
- [26] S.J. Weiner, P.A. Kollman, D.A. Case, U.C. Singh, C. Ghio, G. Alagona, S. Profeta Jr., P.J. Weiner, *Am. Chem. Soc.* 106, 765–784 (1984).
- [27] J. Wang, P. Cieplak, P.A. Kollman, *J. Comput. Chem.* 21, 1049–1074 (2000).
- [28] J. Wang, R.M. Wolf, J.W. Caldwell, P.A. Kollman, D.A. Case, *J. Comput. Chem.* 25, 1157–1174 (2004).
- [29] N.L. Allinger, *J. Am. Chem. Soc.* 99, 8127 (1977).
- [30] N.L. Allinger, Y.H. Yuh, J.-H. Lii, *J. Am. Chem. Soc.* 111, 8551–8566 (1989).
- [31] W.L. Jorgensen, J. Tirado-Rives, *J. Am. Chem. Soc.* 110, 1657–1666 (1988).
- [32] M. Clark, R.D. Cramer III, N. van Opdenbosch, *J. Comput. Chem.* 10, 982 (1989).
- [33] B.R. Brooks, R.E. Bruccoleri, B.D. Olafson, D.J. States, S. Swaminathan, M. Karplus, *J. Comput. Chem.* 4, 187–217 (1983).
- [34] S. Lifson, A.T. Hagler, P. Dauber, *J. Am. Chem. Soc.* 101, 5111–5121 (1979).

- [35] M.J. Hwang, T.P. Stockfish, A.T. Halgler, *J. Am. Chem. Soc.* 116, 2515–2525 (1994).
- [36] F.M. Momany, R. Rone, *J. Comput. Chem.* 13, 888–900 (1992).
- [37] S.L. Mayo, B.D. Olafson, W.A. Goddard III, *J. Phys. Chem.* 94, 8879 (1990).
- [38] A.K. Rappe', C.J. Casewit, K.S. Colwell, W.A. Goddard III, W.M. Skiff, *J. Am. Chem. Soc.* 114, 10024–10035 (1992).
- [39] T.A. Halgren, *J. Comput. Chem.* 17, 490–519 (1996).
- [40] T.A. Halgren, *J. Comput. Chem.* 17, 520–552 (1996).
- [41] T.A. Halgren, *J. Comput. Chem.* 17, 553–586 (1996).
- [42] T.A. Halgren, *J. Comput. Chem.* 17, 587–615 (1996).
- [43] T.A. Halgren, *J. Comput. Chem.* 17, 615–641 (1996).
- [44] T.A. Halgren, *J. Comput. Chem.* 20, 730–748 (1999).
- [45] URL - <http://www.amber.ucsf.edu/amber/amber.html>
- [46] URL - <http://www.lobos.nih.gov/Charmm>
- [47] HyperChem 8.0 (*Molecular Modeling System*) Hypercube, Inc. USA, (2007).
- [48] S.Lifson, A.Warshel, *J. Chem. Phys.* 49, 5116–5129 (1968).

- [49] A. Warshel, S. Lifson, *J. Chem. Phys.* 53, 582–594 (1970).
- [50] A. Warshel, M. Levitt, S. Lifson, *J. Mol. Spectrosc.* 33, 84–99 (1970).
- [51] O. Ermer, S. Lifson, *J. Am. Chem. Soc.* 95, 4121–4132 (1973).
- [52] S. L. Mayo, B. D. Olafson and W. A. Goddard III, *J. Chem. Phys.* 94, 8897 (1990).
- [53] T. A. Halgren, *J. Computational Chem.* 17, 490 (1996).
- [54] J. E. Bol, C. Buning, P. Comba, J. Reedijk, M. Stro ¨hle, *J. Comput. Chem.* 19, 512 (1998).
- [55] <http://www.igc.ethz.ch/GROMOS/index>
- [56] W. F. van Gunsteren, & H. J. C. Berendsen, *Mol. Phys.* 34, 1311–1327 (1977).
- [57] B. A. C. Horta, P. F. J. Fuchs, W. F. van Gunsteren, & P. H. Hunenberger. *J. Chem. Theory Comp.* 7, 1016–1031 (April 2011).
- [58] C. Altona, and D. H. Faber, *Top. Curr. Chem.* 45, 1–38 (1974).
- [59] K. B. Wiberg, *J. Am. Chem. Soc.* 87, 1070–1078 (1965).

- [60] [K. Williamson](#), [K. Masters](#) , Macroscale and Microscale Organic Experiments,
6thed. Éditeur Cengage Learning, usa (2010).

CHAPITRE II:

**Computational Methods Applied in
Physical-Chemistry property/activity
Relationships of Thiophene Derivatives**

1. INTRODUCTION

Thiophene derivatives represent important building blocks in organic and medicinal chemistry. In addition they are of interest in their own right due to their pharmacological properties. For example, 5-substituted 2-aminothiophenes and amino-5-bromo-4-(3-nitrophenyl) thiophene are A1 adenosine receptor agonists¹⁻². Also, many thieno[2,3-d]pyrimidine derivatives were covered by patents as phosphor-diesterase inhibitors³ and various receptor antagonists⁴⁻⁵. Various thieno[2,3-d]pyrimidine derivatives show pronounced anti-tumor⁶ and radioprotective activities⁷. Based on thieno[2,3-d] pyrimidine derivatives immunomodulators⁸ and compounds used for prophylaxis and therapy of cerebral ischemia,⁹ malaria,¹⁰⁻¹² tuberculosis,¹³ Alzheimer's disease,¹⁴ Parkinson's disease,¹⁵ and other diseases were designed^{16,17}.

Thiophene derivatives have been reported to possess broad spectrum of biological properties including anti-inflammatory¹⁸, analgesic¹⁹, antidepressant²⁰, antimicrobial²¹ and anticonvulsant activities²²⁻²⁵. Presently available active antiepileptic drugs (AEDs) like tiagabine²², etizolam²⁴, brotizolam²⁵ are containing thiophene moiety in their

structures as active pharmacophore. Also, it has been established that the higher activity of sodium phethenylate²³ is due to the presence of thiophene ring in its structure.

Further, compounds containing hydrazones and thiosemicarbazones with different types of substitution are well documented for their anticonvulsant activity²⁶⁻³¹.

Quantum chemistry methods play an important role in obtaining molecular geometries and predicting various properties³². To obtain highly accurate geometries and physical properties for molecules that are built from electronegative elements, expensive Ab initio/HF electron correlation methods are required³³⁻³⁶. Density functional theory methods offer an alternative use of inexpensive computational methods which could handle relatively large molecules³⁷⁻⁴⁴.

Quantitative Structure-Activity Relationships (QSAR) are attempts to correlate molecular structure or properties derived from molecular structure with a particular kind of chemical or biochemical activity⁴⁵⁻⁴⁷. The kind of activity is a function of the user's⁴⁸ interest. QSAR is a predictive tool for a preliminary evaluation of the activity of chemical compounds by using computer aided models⁴⁹⁻⁵². QSAR is widely used in pharmaceutical, environmental, and agricultural chemistry in the search for particular

properties. The molecular properties used in the correlations relate as directly as possible to key physical or chemical processes taking place in the target activity⁴⁸.

Quantitative structure activity relationship techniques increase the probability of success and reduce time and cost in drug discovery process⁴⁹⁻⁵². QSAR has done much to enhance our understanding of fundamental processes and phenomena in medicinal chemistry and drug design⁵³⁻⁵⁷. This paper deals with a specific organization form of molecular matter. Other forms are given for example in the references⁵⁸⁻⁶⁴.

Drug-likeness is a qualitative concept used in drug design, which is estimated from the molecular structure before the substance is even synthesized and tested. The calculation of drug-like property can give us better assumption of biological activity of certain molecule. The theoretical calculation of certain properties of a molecule can fill the parameters, which are essential to show certain biological activity.⁶⁵

The term drug-like captures the concept that certain properties of compounds are most advantageous in their becoming successful drug products. The term became commonly used following the pivotal work of Lipinski and his colleagues at Pfizer⁶⁶. Their work examined the structural properties that affect the physicochemical properties

of solubility and permeability and their effect on drug absorption. The term *drug-like property* has expanded and has been linked to all properties that affect ADME/Tox.

Although medicinal chemists and pharmaceutical scientists had used structural properties in various ways for many years, *rules* became more prominent and defined in the field with the report by Lipinski et al⁶⁶ of the “rule of 5,” or what has become known as the “Lipinski rules.” These rules are a set of property values that were derived from classifying key physicochemical properties of drug-like compounds. The rule of five is based on four properties of molecules; namely, molecular weight (MW), logP, number of hydrogen-bond donors (HBD) taken as equivalent to the number of –OH and –NH groups, and the number of hydrogen-bond acceptors (HBA) taken as equivalent to the number of oxygen and nitrogen atoms. A ‘flag’ is set if a molecule’s MW is greater than 500, its logP is greater than 5, the number of its HBDs exceeds 5 and the number of its HBAs exceeds 10. Because the values of the decision points for all of the property values are multiples of five, the above set of rules has been called the ‘Rule of Five’⁶⁶.

2. MATERIALS AND METHODS

All calculations were performed by using HyperChem 8.0.6 software⁶⁷ and Gaussian 09 program package⁶⁸. The geometries of thiophene and their methyl, chloro derivatives, and the series of thiophene derivatives were fully re-optimized by a PM3 method. A parallel study has been made using Ab initio/HF, MP2 and DFT/B3LYP exchange-correlation potential with 6-311+G(d,p) basis⁶⁹⁻⁷⁰. The calculation of QSAR properties is performed by the module QSAR Properties, (version 8.0.6). QSAR Properties is a module, that together with HyperChem, allows several properties commonly used in QSAR studies to be calculated. The calculations are empirical and, so generally, are fast. The calculated results have been reported in the present work.

3. RESULTS AND DISCUSSION

3.1. Electronic Structure of thiophene and thiophene systems

3.1.1. Electronic structure of thiophene

The efficiency of DFT/B3LYP method may be scrutinized by comparison with the results obtained by more elaborate calculation such as Ab initio and MP2. Results concerning bond length values for thiophene are in Table 1, bond angles in Table 2, and

charge densities in Table 3. We found good agreement between predicted geometries (bond lengths and bond angles) and corresponding experimental data, especially the DFT/B3LYP results. From that, we can say the DFT method is more appropriate for further study on thiophene ring. Charge densities calculated by DFT/B3LYP are almost similar to Ab initio/HF and MP2 methods. The geometry of the thiophene is planar; dihedral angles are almost equal to zero.

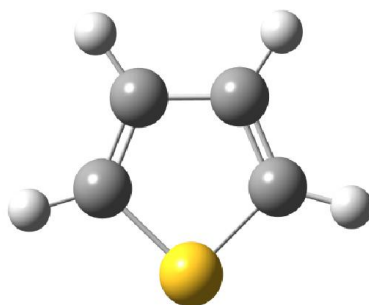


Fig.1 3D conformation of thiophene (GaussView 5.0.8)

Table 1 Calculated bond lengths (angstrom) of thiophene molecule

Distance	EXP ⁷¹⁻⁷²	PM3	Ab initio/HF /6-311+G(d,p)	DFT/B3LYP /6-311+G(d,p)	MP2 /6-311+G(d,p)
S1-C2	1.714	1.725	1.724	1.736	1.712
C2-C3	1.370	1.365	1.346	1.367	1.382
C3-C4	1.432	1.436	1.436	1.430	1.421
C2-H2	1.078	1.088	1.071	1.081	1.082
C3-H3	1.081	1.090	1.074	1.084	1.084

PM3 (Hyperchem8.0.6), Ab initio, MP2 and DFT (Gaussian09)

Table 2 Angles in degree of thiophene molecule

Angle	EXP ⁷¹⁻⁷²	PM3	Ab initio/HF /6-311+G(d,p)	DFT/B3LYP /6-311+G(d,p)	MP2 /6-311+G(d,p)
S1-C2-C3	111.5	112.1	111.8	111.5	111.7
C2-C3-C4	112.5	112.2	112.5	112.7	112.2
C2-S1-C5	92.2	91.4	91.3	91.5	92.2
H2-C2-S1	119.9	122.4	120.4	120.1	120.2
H3-C3-C2	123.3	124.9	123.6	123.3	123.2

PM3 (Hyperchem8.0.6), Ab initio, MP2 and DFT (Gaussian09)

Table 3 Net charge distribution for thiophene molecule

Thiophene atoms	Ab initio/HF /6-311+G(d,p)	DFT/B3LYP /6-311+G(d,p)	MP2 /6-311+G(d,p)
S1	0.007	0.029	0.034
C2	-0.101	-0.128	-0.122
C3	-0.220	-0.189	-0.219
C4	-0.220	-0.189	-0.219
C5	-0.101	-0.128	-0.122

Ab initio, DFT and MP2 (Gaussian09)

The molecular electrostatic potential MESP yields information on the molecular regions that are preferred or avoided by an electrophile or nucleophile. Any chemical system creates an electrostatic potential around itself. When a hypothetical ‘volumeless’ unit positive charge is used as a probe, it feels the attractive or repulsive forces in regions where the electrostatic potential is negative or positive respectively⁷³. It has been found to be a very useful tool in the investigation of the correlation between the molecular structure and the physiochemical property relationship of molecules including biomolecules and drugs⁷³⁻⁷⁷. The red and blue regions in the MESP map refer to regions of negative and positive potential and correspond to electron rich and

electron-deficient regions respectively, whereas the green color signifies neutral electrostatic potential⁷⁸.

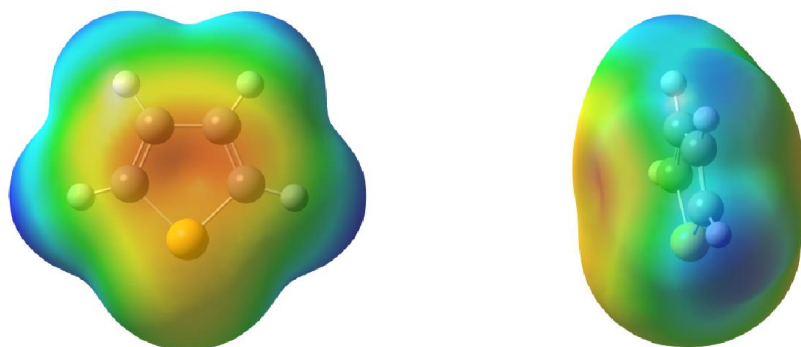


Fig.2 Two views of 3D MESP surface of thiophene (GaussView 5)

The MESP surface map for thiophene shows that the region near the carbon atoms is rich with electrons due to the red color that refers to a negative potential. In the other hand, the region around the sulfur atom is more orange or yellow which indicates a less negative potential than the previous one. The green region refers to a neutral electrostatic potential, but the blue small regions signifies a slight deficient in electrons compared to the four major positive potential regions around each Hydrogen atom characterized by the dark blue color, which indicates that these regions bear the maximum brunt of positive charges.

3.1.2. Electronic Structure of substituted thiophenes

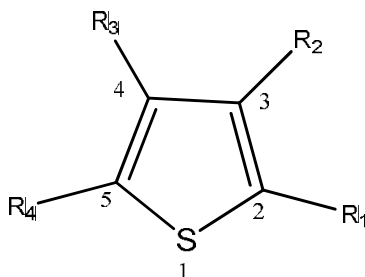


Fig.3 Scheme of thiophene systems.

Calculated values of methyl substituted thiophenes and chloride substituted thiophenes (Figure 2) are given in Tables 4-7. In Tables 4-5, heat of formation, dipole moment, HOMO (highest occupied molecular orbital), LUMO (lowest unoccupied molecular orbital) and their difference (ΔE) are reported for thiophene and its methyl and chloride derivatives. Net atomic charges are reported in Tables 6-7.

	Series 1		Series 2
1	$R_1=R_2=R_3=R_4=H$	1	$R_1=R_2=R_3=R_4=H$
2	$R_1=CH_3, R_2=R_3=R_4=H$	2	$R_1=Cl, R_2=R_3=R_4=H$
3	$R_3=CH_3, R_1=R_2=R_4=H$	3	$R_3=Cl, R_1=R_2=R_4=H$
4	$R_1=R_2=CH_3, R_3=R_4=H$	4	$R_1=R_2=Cl, R_3=R_4=H$
5	$R_1=R_3=CH_3, R_2=R_4=H$	5	$R_1=R_3=Cl, R_2=R_4=H$
6	$R_1=R_4=CH_3, R_2=R_3=H$	6	$R_1=R_4=Cl, R_2=R_3=H$
7	$R_2=R_3=CH_3, R_1=R_4=H$	7	$R_2=R_3=Cl, R_1=R_4=H$
8	$R_1=R_2=R_3=CH_3, R_4=H$	8	$R_1=R_2=R_3=Cl, R_4=H$
9	$R_1=R_2=R_4=CH_3, R_3=H$	9	$R_1=R_2=R_4=Cl, R_3=H$
10	$R_1=R_2=R_3=R_4=CH_3$	10	$R_1=R_2=R_3=R_4=Cl$

It can be seen from the heat of formation data that approximately 8 kcal/mol is decreased at each addition of methyl group, in the base compound thiophene irrespective of the number of substitutions.

The ionization potential values in compounds (1-10) shows a decreasing trend, which means increasing trend in the easy flow of charges in higher energy states of these compounds.

The atomic charge of sulfur is decreased for methyl derivatives and increased for chloride derivatives. However, in the methyl derivatives, the decrease is most important.

In the mono-substituted methyl group category, the 2-methyl thiophene (compound 2) shows a maximum charge on the 5th position carbon (-0.300), which leads to the electrophilic substitution (Table 6). This is further supported by the least HOMO-LUMO energy gap (0.226) as in Table 4, which depicts the chemical reactivity of the compound; the higher the HOMO-LUMO energy gap the lesser is the flow of electrons to the higher energy state making the molecule hard and less reactive. On the other hand, in lesser HOMO-LUMO gap, there is an easy flow of electrons to the higher energy state making it softer and more reactive (HSAB principle: hard and soft acids

and bases). Hard bases have HOMO of low energy, and hard acids have LUMO of high energy⁷⁹. Compound 2 also shows a high dipole moment value compared to the thiophene molecule.

In the case of dimethyl substituted thiophenes, compound 6 presents the least HOMO-LUMO energy gap (0.21) translating to better reactivity. Carbons C4 and C5 positions show a maximum negative charge (-0.151), which leads to preferential site of electrophilic attack (Tables 4-6).

C-H hyper-conjugation is the principal mode of electron release by the methyl group and leads to more stable excited states than the ground state.⁸⁰ In the order of increasing number of conjugated methyl groups, ionization potentials (IPs) decrease in the case of compounds (1-10) as expected from those listed in Table 6.

The 2,3,4,5-tetramethyl thiophene (compound 10) is predicted to be the most reactive with the least HOMO-LUMO energy gap (0.200) of all the thiophene systems and respectively C3 and C4 are the most preferential sites for nucleophilic attack whereas C2 and C5 for electrophilic attack (Table 4). We found in literature that the majority of tetra-substituted thiophenes have biological activity.⁶⁻³¹

We also note that the methyl substituent (donor effect) slightly increases the energy of HOMO with little change in decreasing the one of LUMO (Table 4).

In the present work, we have also studied chloro-substituted thiophenes along the same line of methyl substituted thiophenes for a comparative study. We notice a decrease in the heat of formation, which is approximately 3 kcal/mol for each addition in the 2 and 5 positions, and 6 kcal/mol for each addition in the 3 and 4 positions.

In mono-substituted chloride derivatives, 2-chloro-thiophene (compound 2) is predicted to be more chemically reactive than 3-chloro-thiophene on the basis of least HOMO-LUMO energy gap (Table 5). The carbon 5 in 2-chloro-thiophene shows a maximum negative charge (-0.306) leading to a favored site for electrophilic attack (Table 6).

In dichloride substituted derivatives, 2 and 5-dichloro thiophene (compound 6) seems to be more reactive than the other three compounds 4,5 and 7 due to the least HOMO-LUMO energy gap (0.2706) (Table 5). Carbons C2 and C5 positions show a maximum negative charge (-0.307), which leads to preferential site of electrophilic attack (Tables 5-7). We note that the chloride substituent (attractor effect) lowers the

energies of HOMO and LUMO. Its influence on the energy of the LUMO is more important (Table 5). Also for each chloride substituted in the thiophene ring, we notice an increase in the gap HOMO-LUMO so the chloride substituted compounds are more stable and less reactive compared to the thiophene and the other studied compounds.

After the chloride substitutions we notice that all the carbons took a negative charge, which means that the chloro-substituted compounds favored only the electrophilic attacks.

Table 4 Energies of thiophene and methyl-substituted thiophenes.

Compound	ΔH_f (au)	HOMO (au)	LUMO (au)	ΔE (au)	M (Debye)
1 Thiophene	30.6097	-0.2333	0.0084	0.2417	0.6230
2 2-methyl thiophene	23.0443	-0.2218	0.0050	0.2268	0.7291
3 3-methyl thiophene	21.1110	-0.2249	0.0068	0.2317	0.9472
4 2,3-dimethyl thiophene	13.7894	-0.2154	0.0016	0.2170	1.0280
5 2,4-dimethyl thiophene	13.5569	-0.2144	0.0036	0.2180	0.9012
6 2,5-dimethyl thiophene	15.6469	-0.2093	0.0014	0.2107	0.4562
7 3,4-dimethyl thiophene	11.6034	-0.2228	0.0015	0.2243	1.2874
8 2,3,4-trimethyl thiophene	4.5235	-0.2116	0.0058	0.2174	1.2315
9 2, 3,5-trimethyl thiophene	6.3558	-0.2051	0.0059	0.2110	0.7597
10 2, 3, 4,5-tetramethyl thiophene	-2.4759	-0.2000	0.0002	0.2002	1.0091

ΔH_f calculated by PM3 (Hyperchem8.0.6) HOMO, LUMO, ΔE , μ calculated by DFT (Gaussian09)

Table 5 Energies of thiophene and chloride-substituted thiophenes.

	Compound	ΔH_f (au)	HOMO (au)	LUMO (au)	ΔE (au)	M(Debye)
1	Thiophene	30.6097	-0.2333	0.0084	0.2417	0.6230
2	2-chloro thiophene	27.6163	-0.2335	-0.0228	0.2563	1.7848
3	3-chloro thiophene	24.4915	-0.2407	-0.0232	0.2639	1.4004
4	2,3-dichloro thiophene	22.0610	-0.2404	-0.0340	0.2744	2.2492
5	2,4-dichloro thiophene	21.6609	-0.2420	-0.0361	0.2781	0.6646
6	2,5-dichloro thiophene	24.7989	-0.2349	-0.0357	0.2706	1.2480
7	3,4-dichloro thiophene	19.3164	-0.2509	-0.0344	0.2853	2.0288
8	2, 3,4-trichloro thiophene	16.9437	-0.2480	-0.0444	0.2924	1.8768
9	2,3,5-trichloro thiophene	19.3748	-0.2414	-0.0458	0.2872	0.7645
10	2, 3, 4,5-tetrachloro thiophene	14.7041	-0.2465	-0.0533	0.2998	1.0243

ΔH_f calculated by PM3 (Hyperchem8.0.6) HOMO, LUMO, ΔE , μ by calculated DFT (Gaussian09)

Table 6 Net atomic charges for methyl-substituted thiophenes.

Compound	1	2	3	4	5	6	7	8	9	10
Sulfur 1	0.521	0.230	0.245	0.226	0.224	0.223	0.233	0.220	0.213	0.200
Carbon-2	-0.298	-0.137	-0.337	-0.194	-0.139	-0.151	-0.343	-0.199	-0.197	-0.188
Carbon-3	-0.052	-0.068	0.140	0.135	-0.084	-0.068	0.131	0.123	0.135	0.116
Carbon-4	-0.052	-0.051	-0.066	-0.069	0.145	-0.068	0.131	0.130	-0.083	0.116
Carbon-5	-0.298	-0.300	-0.302	-0.303	-0.342	-0.151	-0.343	-0.347	-0.152	-0.188
C-methyl-2	-	-0.357	-	-0.352	-0.358	-0.354	-	-0.351	-0.354	-0.361
C-methyl-3	-	-	-0.377	-0.377	-	-	-0.373	-0.377	-0.378	-0.383
C-methyl-4	-	-	-	-	-0.378	-	-0.373	-0.373	-	-0.383
C-methyl-5	-	-	-	-	-	-0.354	-	-	-0.353	-0.361

Net charge calculated by DFT (Gaussian09)

Table 7 Net atomic charges for chloride-substituted thiophenes.

Compound	1	2	3	4	5	6	7	8	9	10
Sulfur 1	0.521	0.302	0.280	0.325	0.328	0.351	0.306	0.347	0.370	0.387
Carbon-2	-0.298	-0.299	-0.295	-0.305	-0.302	-0.307	-0.296	-0.306	-0.314	-0.313
Carbon-3	-0.052	-0.034	-0.057	-0.043	-0.008	-0.029	-0.042	-0.027	-0.038	-0.023
Carbon-4	-0.052	-0.046	-0.027	-0.022	-0.053	-0.029	-0.042	-0.037	-0.004	-0.023
Carbon-5	-0.298	-0.306	-0.301	-0.307	-0.304	-0.307	-0.296	-0.304	-0.309	-0.313
Chloro-2	-	0.026	-	0.056	0.042	0.037	-	0.068	0.066	0.076
Chloro-3	-	-	-0.007	0.026	-	-	0.029	0.060	0.037	0.067
Chloro-4	-	-	-	-	0.006	-	0.029	0.037	-	0.067
Chloro-5	-	-	-	-	-	0.037	-	-	0.051	0.076

Net charge calculated by DFT (Gaussian09)

3.2. Study of structure and physical-chemistry activity relationship for thiophene derivatives

We have studied seven physical-chemistry properties of thiophene derivatives using HyperChem. We will continue this work in the future by a quantitative calculation. These properties are: van der Waals-surface-bounded molecular volume, the log of the octanol-water partition coefficient (log p), polarizability, solvent-accessible surface bounded molecular volume, molecular mass, hydration energy and molar refractivity.

Calculation of log P is carried out using atomic parameters derived by Ghose and coworkers⁸¹. Computation of molar refractivity was made via the same method as log p. Ghose and Crippen presented atomic contributions to the refractivity⁸². Solvent-accessible surface bounded molecular volume and van der Waals-surface-bounded molecular volume calculations are based on a grid method derived by Bodor et al⁸³, using the atomic radii of Gavezzotti⁸⁴.

Polarizability was estimated from an additivity scheme given by Miller⁸⁵ with a 3% in precision for the calculation, where different increments are associated with different atom types. Hydration energy is a key factor determining the stability of different molecular conformations⁸⁶. The calculation is based on exposed surface area, and employs the surface area as computed by the approximate method (above), weighted by atom type.

3.2. 1. Structural comparison of thiophene derivatives

Based on our conclusions on the effect of substitution on the thiophene molecule, we chose a series of thiophene derivatives (thiophene-2,5 dicarbohydrazides); these molecules possess a biological activity. The present series of thiophene derivatives have been synthesized and characterized by Ravi Kulandasamy et al⁸⁷. Initially, we performed a structural comparison of this series Figure 4. For example, Figure 5 shows the favored conformation in 3D of the compound C1. These molecules have a weak conformational flexibility, with regard to the other macrocycles of macrolide type⁸⁸⁻⁹⁴. In a window of 2kcal/mol, only one favored conformations is found, for each structure.

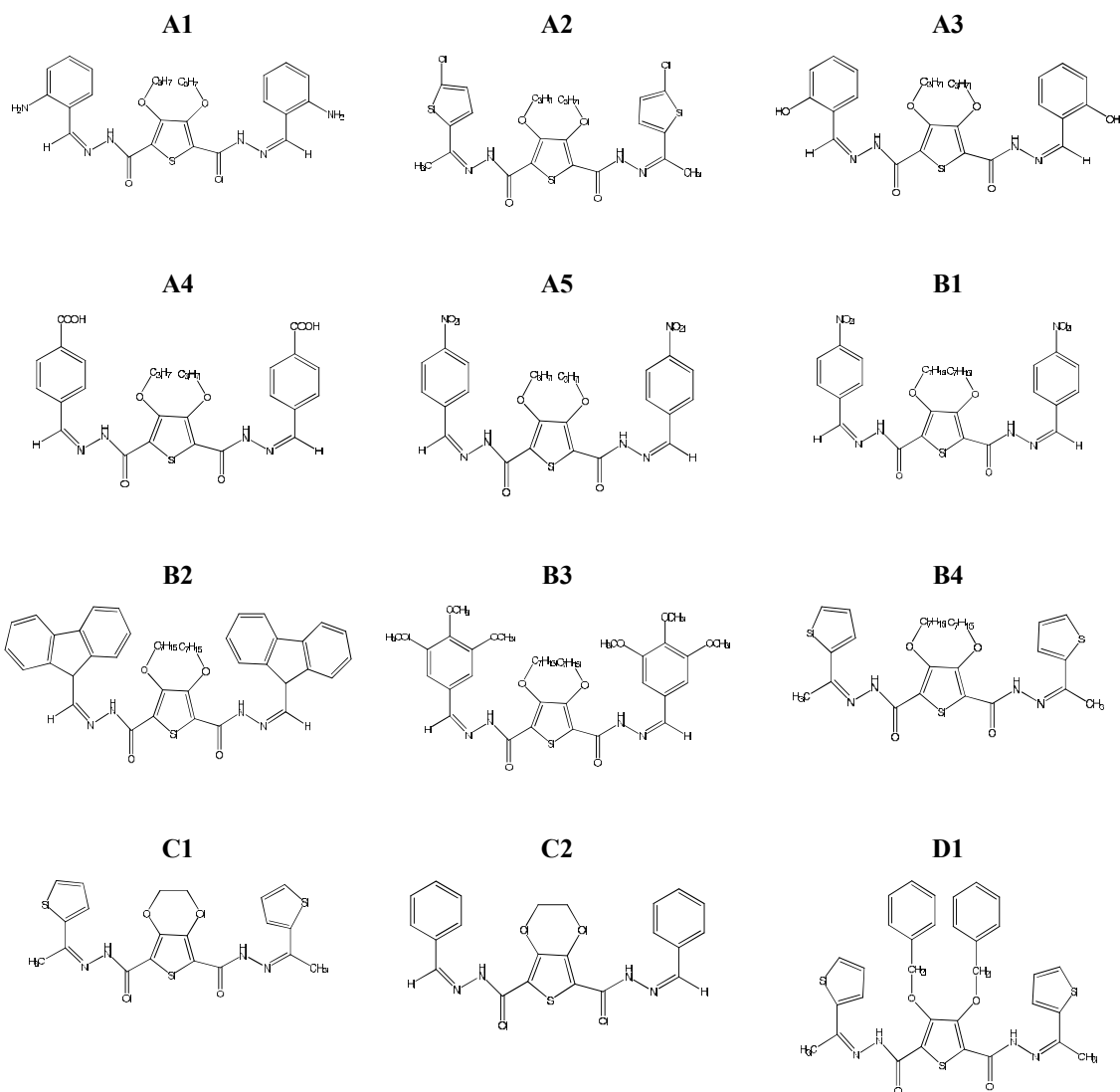


Fig.4 Structural comparison of the thiophene derivatives

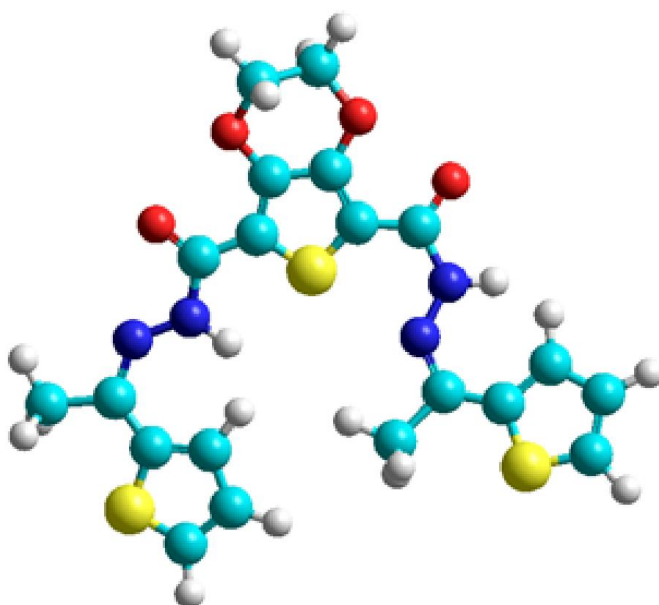


Fig.5 3D Conformation of compound C1 (HyperChem 8.0.6)

3.2. 2. Structure and physical-chemistry activity relationship

Polarizability values are generally proportional to surfaces and of volumes. The decreasing order of polarizability for these studied thiophenes is: B2, B3, B1, B4, D1, A2, A4, A5, A1, A3, C1, and C2 (Table 8). The order of polarizability is the same one for the mass, but it is a little different for surfaces and volumes. This is due primarily to the folding of surfaces of some structures compared to the majority of the extended

structures. This also is explained by the relation between the polarizability and the volume for the relatively non polar molecules.

Table 8 QSAR proprieties for thiophene derivatives

thiophene derivative	Molecular Mass (uma)	Molecular Surface (\AA^2)	Molecular Volume (\AA^3)	Polarizability (\AA^3)	Hydratation energy (Kcal/mol)	Refractivity (\AA^3)	(Log P)
C-2	434.47	642.85	1123.87	45.53	-13.36	128.92	-2.04
C-1	474.57	647.35	1130.01	48.24	-11.69	132.47	-2.90
A-3	524.59	779.03	1380.43	54.92	-20.95	152.65	-2.29
A-1	522.62	831.82	1417.44	56.34	-17.61	156.54	-3.68
A-5	582.59	835.69	1478.40	57.34	-32.50	163.11	-1.62
A-4	580.61	834.48	1482.53	58.76	-21.06	161.43	-1.47
A-2	601.58	805.18	1444.25	60.21	-8.48	162.79	1.18
D-1	628.78	806.19	1509.75	68.34	-11.01	191.94	-0.70
B-4	644.91	954.95	1745.92	71.04	-6.15	189.79	2.07
B-1	694.80	1015.35	1849.21	72.02	-30.19	199.91	1.55
B-3	784.96	1135.45	2137.29	83.15	-12.16	224.49	-3.03
B-2	781.02	1197.85	2200.91	89.76	-7.25	248.08	2.85

All proprieties calculated by HyperChem 8.0.6

The polarizability of the molecule depends only on its volume, which means that thermal agitation of non-polar molecules does not have any influence on the appearance of dipole moments in these molecules. On the other hand, for polar molecules, the polarizability of the molecule does not depend solely on the volume but also depends on other factors such as the temperature because of the presence of the permanent dipole⁹⁵.

Surface and volume distribution of these molecules are definitely higher than that of more polar molecules like the lipopeptides or beta-lactams. For example, Deleu et al. used TAMMO software⁹⁶ on the surfactins C13, C14 and C15 having cores similar to the macrolides. They found that their surfaces vary from 129 to 157 Å²(see 97), contrarily to these thiophenes, surfaces vary from 642.85 to 1197.85 Å². These thiophenes have a great variation of volume distribution. In particular, compounds B3 and B2 have volumes 2137.29 and 2200.91 Å³ respectively as shown in Table 7.

The most important hydration energy in the absolute value is that of compound A5 32.50 kcal/mol and the weakest is that of compound B4 6.15 kcal/mol (Table 7). Indeed, in biological environments, the polar molecules are surrounded by water molecules. They establish hydrogen bonds between water molecule and these ones. The donor sites of proton interact with the oxygen atom of water and the acceptor sites of proton interact with the hydrogen atom. The first corresponds to the composite with the strongest hydrogen bond. These hydrated molecules were dehydrated at least partially before and at the time of their interaction. These interactions of weak energy, which we observe in particular between messengers and receivers, are generally reversible⁹⁸.

Compound A5 has two donor sites of proton (2 NH) and fifteen acceptor sites of proton (8O, 6N and 1S). On the other hand, compound B4 has two donor sites of proton (2 NH), but possesses only eleven acceptor sites of proton (4O, 4N and 3S). The first compound has four more donor sites of protons, which mean higher value. This property supports the first compound, not only by fixing on the receiver, but also activates it more. It is thus an agonist. It has as a consequence of a better distribution in fabrics.

Lipophilicity is a property that has a major effect on solubility, absorption, distribution, metabolism, and excretion properties as well as pharmacological activity. Lipophilicity has been studied and applied as an important drug property for decades. It can be quickly measured or calculated. Lipophilicity has been correlated to many other properties, such as bioavailability, storage in tissues, permeability, volume of distribution, toxicity, plasma protein binding and enzyme receptor binding^{99,100}.

Log P values of compounds A-2, B-1, B-2 and B-4 are in the field of optimal values ($0 < \text{Log P} < 3$). From that, we can say that these compounds have a good oral

bioavailability and optimal biological activity. For log P too high, the drug has low solubility and for log P too low, the drug has difficulty penetrating lipid membranes⁹⁹.

Compound A1 presents low coefficient of division Log P (-3.68) and comes after compound B3 (-3.03) and C1 (-2.90). These molecules possess a good solubility. When the coefficient of division is rather low, it has as a consequence of a better gastric tolerance. Compounds B2 and B4, which have respectively higher values (2.85) and (2.07) are the most absorbent products and have important capacities to bind on plasmatic proteins.

3.2. 3. Drug-like calculation on the basis of Lipinski rule of five

Drug-like appears as a promising paradigm to encode the balance among the molecular properties of a compound that influences its pharmacodynamics and pharmacokinetics and ultimately optimizes their absorption, distribution, metabolism and excretion (ADME) in human body like a drug. The empirical conditions to satisfy Lipinski's rule and manifest a good oral bioavailability involve a balance between the aqueous solubility of a compound and its ability to diffuse passively through the different biological barriers^{66,101}. These parameters allow ascertaining oral absorption or

membrane permeability that occurs when the evaluated molecule follows Lipinski's rule of five since molecular weight ($MW \leq 500$ Da), an octanol-water partition coefficient $\log P \leq 5$, H-bond donors, nitrogen or oxygen atoms with one or more hydrogen atoms (HBD) ≤ 5 and H-bond acceptors, nitrogen or oxygen atoms (HBA) ≤ 10 .

Molecules that violate more than one of these rules may have problems with bioavailability. Therefore, this rule establishes some structural parameters relevant to the theoretical prediction of the oral bioavailability profile, and is widely used in designing new drugs. However, classes of compounds that are substrates for biological transporters such as antibiotics, antifungals, vitamins, and cardiac glycosides, are exceptions to the rule⁶⁶. The total number of violations is the ROF-Score, which lies between 0 and 4¹⁰².

The calculation results (Table 9) show that most of the studied compounds (C2, C1, A3, A1, A2, D1, B4, B2) agree with Lipinski rules with ROF- violation ≤ 1 , suggesting that these compounds theoretically would not have problems with oral bioavailability except compounds A5, A4, B1, and B2, which have ROF-Score equal to 2; Molecules with ROF-Scores greater than one are considered to be marginal for further

development. Although, as pointed out by Lipinski and co-workers⁶⁶, such molecules should not necessarily be removed from further consideration, but rather, they should be deprioritized in the discovery research process.

Lastly, it is well known that many drugs violate the ROF, but this is not a serious issue since it was not originally designed as a tool for assessing drug likeness.

Nevertheless, its common usage for this purpose has, de facto, made it so in practice.

Table 9 Lipinski's rule of five for drug likeliness of thiophene derivatives

thiophene derivative	Molecular Mass (uma)	(Log P)	HBD	HBA	Rule of five violations
C-2	434.47	-2.04	2	8	0
C-1	474.57	-2.90	2	8	0
A-3	524.59	-2.29	4	10	1
A-1	522.62	-3.68	4	10	1
A-5	582.59	-1.62	2	14	2
A-4	580.61	-1.47	4	12	2
A-2	601.58	1.18	2	8	1
D-1	628.78	-0.70	2	8	1
B-4	644.91	2.07	2	8	1
B-1	694.80	1.55	2	14	2
B-3	784.96	-3.03	2	14	2
B-2	781.02	2.85	2	8	1

MM and Log P calculated by HyperChem 8.0

4. CONCLUSIONS

The study of the methyl and chloride substitution on the thiophene ring shows an influence of the nature of the substituted donor group (methyl) on increasing HOMO energy and decreasing the LUMO energy, and on heat of formation, which is

approximately 8 kcal/mol decreased at each addition of methyl group. Also shows the influence of the substituted acceptor group (chloride) by lowering the energies of HOMO and LUMO and decreasing the heat of formation by 3 kcal / mol for each addition in the 2 and 5 positions and 6 kcal / mol for each addition in the 3 and 4 positions. The present study provides a discussion of several molecular properties of thiophene derivatives based on MP2, Ab initio and density functional theory calculations. Our calculated results are close to the experimental data especially the Density functional theory results. The 2, 3, 4, 5-tetramethyl thiophene is predicted to be the most reactive compound with the least energy gap HOMO-LUMO of all thiophene substituted compounds and respectively carbons C3 and C4 are the most preferential sites for nucleophilic attack, and C2 and C5 for electrophilic attack. Compounds B2 and B4 have higher coefficient of division. These lipophilic compounds penetrate in various membranes, including cellular membranes as well as tissues with high lipid content to arrive at the receptor site. The application of Lipinski rules on the studied thiophene derivatives shows that most of these compounds, theoretically, will not have problems with oral bioavailability.

5. REFERENCES

- [1] L. Aurelio, H. Figler, B. L. Flynn, J. Linden and P. J. Scammells, *Bioorg. Med. Chem.* 16, 1319 (2008).
- [2] H. Lütjens, A. Zickgraf, H. Figler, J. Linden, R. Olsson and P. J. J. Scammells, *Med. Chem.* 46, 1870 (2003).
- [3] A. K. Ghakraborti, B. Gopalakrishnan, M. Elizabeth-Sobhia and A. Malde, *Bioorg. Med. Chem. Lett.* 13, 1403 (2003).
- [4] H. R. G. Jules-Marie and T. C. Marius, *Chem. Abstr.* 138, 238195 (2003).
- [5] H. R. G. Jules-Mariea and T. C. Marius, *Chem. Abstr.* 138, 238194 (2003).
- [6] S. Sasaki, N. Cho, Y. Nara, M. Harada, S. Endo, N. Suzuki, Sh. Furuya and M. J. Fujino, *Med. Chem.* 46, 113 (2003).
- [7] O. M. Nassan, A. Y. Hassan, H. I. Heiba and M. M. Ghorb, *Al-Azhar Bull. Sci.* 8, 435 (1997). *Chem. Abstr.* 130, 110174 (1999).
- [8] H. I. Heiba, M. M. Ghorab, N. E. Amin and L. Ramadan, *Egypt. J. Biotechnol.* 4, 16 (1998), *Chem. Abstr.* 132, 49937 (2000).

- [9] S. Gerd, S. Kurt, L. Wilfred, H. Uta, S. Dorothea, K. Monika, S. Laszlo, E. Franz, G.-L.F. Javi, H. Hans-Peter and U. Liliane, *Chem. Abstr.* 133, 89541 (2000).
- [10] A. Rosowsky, M. Chaykovsky, K. K. N. Chen, M. Lin and E. J. J. Modest, *Med. Chem.* 16, 185 (1973).
- [11] M. Chaykovsky, M. Lin, A. Rosowsky and E. J. J. Modest, *Med. Chem.* 16, 188, (1973).
- [12] A. Rosowsky, K. N. N. Chen and M. J. Lin, *Med. Chem.* 16, 191 (1973).
- [13] M. V. Kapustina, YU. O. Omelkin, I. A. Kharizomenova, V. I. Shvedov and L. N. Felitis, *Khim.-farm. Zh.* 25, 38 (1991), *Pharm. Chem. J.* 25, 7 (1991).
- [14] F. Shuichi and S. Nobuhiro, *Chem. Abstr.* 135, 313627 (2001).
- [15] I. Hirotsune, K. Takashi, N. Eisuke, K. Hidetaka, O. Masamichi, T. Takashi and N. Atsushi, *Chem. Abstr.* 137, 169542 (2002).
- [16] W. Lichen, R. Jinzhi, L. Baolin, L. Jiaxuan and Y. J. Jing, *Zhongguo Yaoke Daxue Xuebao* 29, 331 (1998), *Chem. Abstr.* 130, 139309 (1999).
- [17] B. T. Henry, I. R. John and L. C. Andrew, *Chem. Abstr.* 115, 8821 (1991).

- [18] K.I. Molvi, K.K. Vasu, S.G. Yerande, V. Sudarsanam and N. Haque, *Eur. J. Med. Chem.* 42, 1049-1058 (2007).
- [19] P. Broto, G. Moreau and C. Vandycke, *Eur. J. Med. Chem.* 9, 79-84 (1984).
- [20] B.V. Asthalatha, B. Narayana, K.K. Vijaya Raj and N. Suchetha Kumari, *Eur. J. Med. Chem.* 42, 719-728 (2007).
- [21] N. Satheesha Rai, B. Kalluraya, B. Lingappa, S. Shenoy and V.G. Puranic, *Eur. J. Med. Chem.* 43, 1715-1720 (2008).
- [22] S. Arroyo and J. Salas-Puig, *Rev. Neurol.* 32, 1041-1043 (2001).
- [23] P. James. *Spurlock, Denton*, US Patent 2366221 Jan 2, (1945).
- [24] Z. Polivka, J. Holubek, E. Svatek, J. Metys and M. Protiva, *Collect. Czech. Chem. Commun.* 49, 621-623 (1984).
- [25] H. Noguchi, K. Kitazumi, M. Mori and T. Shiba, *J. Pharm. Sci.* 94, 246-251 (2004).
- [26] H.J. Lankau, K. Unverferth, C. Grunwald, H. Hartenhauer, K. Heinecke, K. Bernoster, R. Dost, U. Egerland and C. Rundfeldt, *Eur. J. Med. Chem.* 41, 1-6 (2006).

- [27] J.R. Dimmock, R.N. Puthucode, J.M. Smith, M. Hetherington, J. Wilson Quail, U. Pugazhenti, T. Lechler and J. P. Stables, *J. Med. Chem.* 39, 3984-3997 (1996).
- [28] J.V. Ragavendran, D. Sriram, S. Patil, I.V. Reddy, N. Bharathwajan, J. Stables and P. Yogeewari, *Eur. J. Med. Chem.* 42, 146-151 (2007).
- [29] P. Yogeewari, R. Thirumurugan, R. Kavya, J.S. Samuel, J. Stables and D. Sriram, *Eur. J. Med. Chem.* 39, (2004).
- [30] S. Gunizkuculguzel, A. Mazi, F. Sahin, S. Qzturk and J. Stables, *Eur. J. Med. Chem.* 38, 1005-1013 (2003).
- [31] R. Thirumurugan, D. Sriram, A. Saxena, J. Stables and P. Yogeewari, *Bioorg. Med. Chem.* 14, 3106-3112 (2006).
- [32] M. Ciobanu, L. Preda, D. Savastru, R. Savastru, and E. M. Carstea, *Quantum Matter.* 2, 60 (2013).
- [33] A. Srivastava, S. Jain, and A. K. Nagawat, *Quantum Matter.* 2, 469-473 (2013).
- [34] A. Srivastava, N. Saraf, and A. K. Nagawat, *Quantum Matter.* 2, 401-407 (2013).
- [35] A. Srivastava, N. Jain, and A. K. Nagawat, *Quantum Matter.* 2, 307-313 (2013).

- [36] W.J. Hehre, *Practical Strategies for Electronic Structure Calculations*, Wave functions", Inc., Irvine, California (1995).
- [37] Chia M. Chang, Hsiao L. Tseng, Abraham F. Jalbout, and Aned de Leon, *J. Comput. Theor. Nanosci*, 10, 527, (2013).
- [38] T. L. Jensen, J. Moxnes, and E. Unneberg, *J. Comput. Theor. Nanosci*, 10, 464 (2013).
- [39] M. Narayanan and A. John Peter, *Quantum Matter*, 1, 53, (2012).
- [40] Gregorio H. Coccoletzi and Noboru Takeuchi *Quantum Matter* 2, 382-387 (2013).
- [41] Medhat Ibrahim and Hanan Elhaes, *Rev. Theor. Sci.* 1, 368-376 (2013).
- [42] E. Chigo Anota, H. Hernández Coccoletzi, and M. Castro, *J. Comput. Theor. Nanosci.* 10, 2542-2546 (2013).
- [43] Faranak Bazooyar, Mohammad Taherzadeh, Claes Niklasson, and Kim Bolton, *J. Comput. Theor. Nanosci.* 10, 2639-2646 (2013).
- [44] E. R. Davidson, *Chemical Reviews*, 91, 649 (1991).
- [45] H. Langueur, K. Kassali, and N. Lebga, *J. Comput. Theor. Nanosci*, 10, 86 (2013).

- [46] N. Melkemi and S. Belaidi, *J. Comput. Theor. Nanosci*, 11, 801 (2014).
- [47] M. Narayanan and A. John Peter, *Quantum Matter*, 1, 53 (2012).
- [48] Y. C. Martin, *Quantitative Drug Design*, Marcel Dekker, New York, NY, USA, (1978).
- [49] A.I. Ageenko and Y.E. Vitorgan, *Vopr. Virusol*, 2, 1599 (1975).
- [50] V.R. Talageri, S.N. Revankar, B.N. Mashelkar and K.I. Ranadive, *Biochem. Biophys*, 8, 79 (1971).
- [51] F.B. Hershey, G. Johnson, S.M. Murphy and M. Schmidt, *Cancer Res*, 26, 265 (1966).
- [52] T.T. Otani and H.P. Morris, *J. Natl. Cancer Inst. (US)*, 47, 1247 (1971).
- [53] J. G. Topliss, *Perspect. Drug Discov. Des*, 1, 253 (1993).
- [54] Zhigao Wang, Fangqiang Wang, Changhua Su, and Yongling Zhang *J. Comput. Theor. Nanosci*. 10, 2323-2327 (2013).
- [55] A. Eghdami and M. Monajjemi , *Quantum Matter*, 2, 324-331 (2013).
- [56] Yong Chen, Di Xu, and Min Yang, *J. Comput. Theor. Nanosci*. 10, 2916-2919 (2013).

- [57] Bin Wu, Xiangjun Kong, Zheng Cao, Yuzhu Pan, Yonggang Ren, Yuanchao Li, Qingwu Yang, and Fenglin Lv, *J. Comput. Theor. Nanosci.* 10, 2403-2410 (2013).
- [58] Aleksander Herman, *Rev. Theor. Sci.* 1, 3-33 (2013).
- [59] E. L. Pankratov and E. A. Bulaeva, *Rev. Theor. Sci.* 1, 58-82 (2013).
- [60] Qinyi Zhao, *Rev. Theor. Sci.* 1, 83-101 (2013).
- [61] Andrei Khrennikov, *Rev. Theor. Sci.* 1, 34-57 (2013).
- [62] N. Paitya and K. P. Ghatak, *Rev. Theor. Sci.* 1, 165-305 (2013).
- [63] D. Fiscaletti, *Rev. Theor. Sci.* 1, 103-144 (2013).
- [64] Medhat Ibrahim and Hanan Elhaes, *Rev. Theor. Sci.* 1, 368-376 (2013).
- [65] J. Mazumder, R. Chakraborty, S. Sen, S. Vadra, B. De and T. K. Ravi, *Der Pharma Chemica*, 1(2), 188-198 (2009).
- [66] C. A. Lipinski, F. Lombardo, B. W. Dominy and P. J. Feeney, *Adv. Drug Deliv. Rev.* 4, 17 (2012).
- [67] HyperChem (Molecular Modeling System) Hypercube, Inc., 1115 NW, 4th Street, Gainesville, FL 32601; USA (2007). <http://www.hyperchem.com>.

- [68] Gaussian 09, Revision B.01, M. J. Frisch, G. W. Trucks, H. B. Schlegel, G. E. Scuseria, M. A. Robb, J. R. Cheeseman, G. Scalmani, V. Barone, B. Mennucci, G. A. Petersson, H. Nakatsuji, M. Caricato, X. Li, H. P. Hratchian, A. F. Izmaylov, J. Bloino, G. Zheng, J. L. Sonnenberg, M. Hada, M. Ehara, K. Toyota, R. Fukuda, J. Hasegawa, M. Ishida, T. Nakajima, Y. Honda, O. Kitao, H. Nakai, T. Vreven, J. A. Montgomery, Jr., J. E. Peralta, F. Ogliaro, M. Bearpark, J. J. Heyd, E. Brothers, K. N. Kudin, V. N. Staroverov, T. Keith, R. Kobayashi, J. Normand, K. Raghavachari, A. Rendell, J. C. Burant, S. S. Iyengar, J. Tomasi, M. Cossi, N. Rega, J. M. Millam, M. Klene, J. E. Knox, J. B. Cross, V. Bakken, C. Adamo, J. Jaramillo, R. Gomperts, R. E. Stratmann, O. Yazyev, A. J. Austin, R. Cammi, C. Pomelli, J. W. Ochterski, R. L. Martin, K. Morokuma, V. G. Zakrzewski, G. A. Voth, P. Salvador, J. J. Dannenberg, S. Dapprich, A. D. Daniels, O. Farkas, J. B. Foresman, J. V. Ortiz, J. Cioslowski and D. J. Fox, Gaussian, Inc., Wallingford CT, (2010).
- [69] M.W. Wong, K.B. Wilberg and M.J. Frisch, *J. Am. Chem. Soc.*, 114, 1645 (1992).
- [70] V. Barone and C. Adamo, *J. Phys. Chem.* 99, 15062 (1995).
- [71] J.S. Kwiatkowski, J. Leszczynski and I. Teca, *J. Mol. Struct.* 451, 436–437 (1997).

- [72] B. Bak, D. Christensen, L. Hansen-Nygaard and J. Rastrup-Andersen, *J. Mol. Spectrosc.* 7, 58 (1961).
- [73] J. S. Murray & K. Sen, *Molecular Electrostatic Potentials, Concepts and Applications*. Elsevier, Amsterdam, (1996).
- [74] Alkorta, I. & J.J. Perez. *Int. J. Quant. Chem.* 57, 123–135 (1996).
- [75] Scrocco, E. & Tomasi, J. *Advances in Quantum Chemistry*, Academic Press. P. Lowdin (Ed.) NewYork (1978).
- [76] F. J. Luque, M. Orozco, P. K. Bhadane & S. R. J. Gadre, *Phys. Chem.* 97, 9380–9384 (1993).
- [77] J. Sponer & P. Hobza, *Int. J. Quant. Chem.* 57, 959–970 (1996).
- [78] S. R. Kumar, N. Vijay, K. Amarendra, P. Onkar & S. Leena, *Research Journal of Recent Sciences* 1, 11-18 (2012).
- [79] G.L. Miessler and D.A. Tarr, *Inorganic Chemistry, 2nd ed. Prentice-Hall*, New Jersey, USA, 181(1999).
- [80] A. Weissberger, *the Chemistry of Heterocyclic Compounds*, John Wiley & Sons, New York, (1993).

- [81] V. N. Viswanadhan, A. K. Ghose, G. N. Revankar, and R. K. Robins, *J. Chem. Inf. Comput. Sci.* 29, 163 (1989).
- [82] K. Ghose and G. M. Crippen, *J. Chem. Inf. Comput. Sci.* 27, 21 (1987).
- [83] N. Bodor, Z. Gabanyi, and C. Wong, *J. Am. Chem. Soc.* 111, 3783 (1989).
- [84] A. Gavezotti, *J. Am. Chem. Soc.* 100, 5220 (1983).
- [85] K. J. Miller, *J. Am. Chem. Soc.* 112, 8533 (1990).
- [86] T. Ooi, M. Oobatake, G. Nemethy and H. A. Scheraga, *Proc. Natl. Acad. Sci. USA*, 84, 3086 (1987).
- [87] R. Kulandasamy, A. V. Adhikari and J. P. Stables *European Journal of Medicinal Chemistry*. 44, 4376–4384 (2009).
- [88] S. Belaidi, A. Dibi, and M. Omari, *Turkish Journal of Chemistry*, 26, 491 (2002).
- [89] S. Belaidi, M. Laabassi, R. Gree, and A. Botrel, *Scientific Study & Research*, 4, 27 (2003).
- [90] S. Belaidi, T. Lanez, M. Omari, and A. Botrel, *Asian Journal of Chemistry*, 17, 859 (2005).

- [91] S. Belaidi, M. Omari, T. Lanez, and A. Dibi, *Journal of the Algerian Society of Chemistry*, 14, 27 (2004).
- [92] S. Belaidi, M. Laabassi, R. Gree, and A. Botrel, *Revue Roumaine de Chimie*, 50, 759 (2005).
- [93] S. Belaidi and D. Harkati, *ISRN Organic Chemistry*, 594242 (2011).
- [94] S. Belaidi and N. Melkemi, *Asian Journal of Chemistry*, 25, 9 (2013).
- [95] B. Yavorski and A. Detlaf, *Checklist of Physics*, Editions Mir, Moscow, 376 (1980).
- [96] TAMMO(*Theoretical Analysis of Molecular Membrane Organization*) Editions CRC Press: Boca Raton, Florida, USA, (1995).
- [97] M. Deleu, *Thesis PhD*, FUSAGX, Belgique, (2000).
- [98] L. B. Kier, *Molecular Orbital Theory in Drug Research*, Academic Press New York, (1981).
- [99] E. H. Kerns and L. Di, *Drug-like Properties: Concepts, Structure Design and Methods: from ADME to Toxicity Optimization*, Academic Press, USA, 43-47 (2008).

[100] V. Pliska, B. Testa, H. van de Waterbeemd, R. Mannhold, H. Kubinyi and H.

Timmerman, *Lipophilicity in Drug Action and Toxicology*, Wiley-VCH, Federal

Republic of Germany (1996).

[101] G. Vistoli, A. Pedretti and B. Testa, *Drug. Discov. Today* 13,(7-8) 285-294

(2008).

[102] J. Petit , N. Meurice , C. Kaiser and G. Maggiora, *Bioorg. Med. Chem.* 20, 5343–

5351 (2012).

CHAPITRE III:

**Predictive Qualitative Structure-
Property / Activity Relationships for
Drug Design in some of
Antimycobacterial Pyrrole derivatives**

1. INTRODUCTION

Pyrrole derivatives are considerable attention of synthetic importance due to their extensive used in drug discovery¹ which is linked to their pharmacological activity such as anti-inflammatory², cytotoxicity³, in vitro cytotoxic activity against solid tumor models⁴, treatment of hyperlipidemias⁵, antitumor agents⁶. The pyrroles containing other heterocyclic derivatives have been reported in synthetic and effective biological importance^{7,8}.

Pyrrole derivatives have biological activity such as COX-1/COX-2 inhibitors⁹ and cytotoxic activity against a variety of marine and human tumor models¹⁰. Quantum chemistry methods play an important role in obtaining molecular geometries and predicting various properties¹¹⁻¹⁴. To obtain highly accurate geometries and physical properties for molecules that are built from electronegative elements, expensive ab initio electron correlation methods are required¹⁵. Density functional theory methods offer an alternative use of inexpensive computational methods which could handle relatively large molecules¹⁶⁻²³.

Qualitative and Quantitative Structure-Activity Relationships (SAR and QSAR) are attempts to correlate molecular structure or properties derived from molecular structure with a particular kind of chemical or biochemical activity²⁴⁻²⁶. The kind of activity is a function of the user's²⁷ interest. QSAR is a predictive tool for a preliminary evaluation of the activity of chemical compounds by using computer aided models²⁸⁻³¹. QSAR is widely used in pharmaceutical, environmental, and agricultural chemistry in the search for particular properties. The molecular properties used in the correlations relate as directly as possible to key physical or chemical processes taking place in the target activity²⁷.

Quantitative structure activity relationship techniques increase the probability of success and reduce time and cost in drug discovery process. QSAR has done much to enhance our understanding of fundamental processes and phenomena in medicinal chemistry and drug design³²⁻³⁶. This paper deals with a specific organization form of molecular matter. Other forms are given for example in the references³⁷⁻⁴³.

Drug-likeness is a qualitative concept used in drug design, which is estimated from the molecular structure before the substance is even synthesized and tested. The

calculation of drug-like property can give us better assumption of biological activity of certain molecule. The theoretical calculation of certain properties of a molecule can fill the parameters, which are essential to show certain biological activity.⁴⁴

The term drug-like captures the concept that certain properties of compounds are most advantageous in their becoming successful drug products. The term became commonly used following the pivotal work of Lipinski and his colleagues at Pfizer⁴⁵. Their work examined the structural properties that affect the physicochemical properties of solubility and permeability and their effect on drug absorption. The term drug-like property has expanded and has been linked to all properties that affect ADME/Tox. Although medicinal chemists and pharmaceutical scientists had used structural properties in various ways for many years, *rules* became more prominent and defined in the field with the report by Lipinski et al⁴⁵ of the “rule of 5,” or what has become known as the “Lipinski rules.” These rules are a set of property values that were derived from classifying key physicochemical properties of drug-like compounds. The rule of five is based on four properties of molecules; namely, molecular weight (MW), logP, number of hydrogen-bond donors (HBD) taken as equivalent to the number of –

OH and –NH groups, and the number of hydrogen-bond acceptors (HBA) taken as equivalent to the number of oxygen and nitrogen atoms. A ‘flag’ is set if a molecule’s MW is greater than 500, its logP is greater than 5, the number of its HBDs exceeds 5 and the number of its HBAs exceeds 10. Because the values of the decision points for all of the property values are multiples of five, the above set of rules has been called the ‘Rule of Five’⁴⁵.

2. MATERIALS AND METHODS

All calculations were performed by using HyperChem 8.0.6 software⁴⁶, Gaussian 09 program package⁴⁷ and Molinspiration online database⁴⁸.

The geometries of pyrrole and their methyl, derivatives, and the series of pyrrole derivatives were fully optimized by a PM3 method. A parallel study has been made using Ab initio/HF, Ab initio/MP2 and DFT/B3LYP exchange-correlation potential with 6-31G(d,p) basis⁴⁹⁻⁵⁰. The calculation of QSAR properties is performed by the module QSAR Properties, (version 8.0.6). QSAR Properties is a module, that together with HyperChem, allows several properties commonly used in QSAR studies to be calculated. The calculated results have been reported in the present work.

3. RESULTS AND DISCUSSION

3.1. *Geometric and Electronic Structure of pyrrole*

The efficiency of PM3 method may be scrutinized by comparison with the results obtained by more elaborate calculation such as ab initio and DFT. Results concerning bond length values for pyrrole are in Table 1, bond angles in Table 2, and charge densities in Table 3.

We found good agreement between predicted geometries (bond lengths and bond angles) and corresponding experimental data, especially the DFT/B3LYP results. From that, we can say the DFT method is more appropriate for further study on pyrrole ring. Charge densities calculated by DFT/B3LYP are almost similar to ab initio/HF and ab initio/MP2 methods. The geometry of the pyrrole is planar; dihedral angles are almost equal to zero.

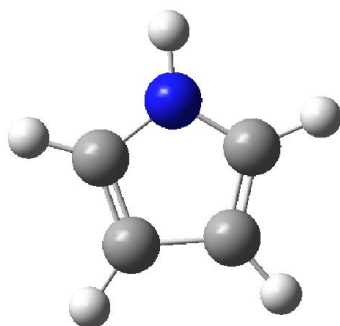


Fig.1 3D conformation of pyrrole (GaussView 5.0.8)

Table 1 Calculated bond lengths (angstrom) of pyrrole molecule

Distance	Exp. ⁵¹	PM3	Ab initio /HF /6-31G(d,p)	DFT/B3LYP /6-31G(d,p)	Ab initio /MP2 /6-31G(d,p)
N1-C2	1.370	1.397	1.362	1.375	1.372
C2-C3	1.382	1.389	1.358	1.378	1.382
C3-C4	1.417	1.421	1.426	1.425	1.418
N1H6	0.996	0.985	0.991	1.002	1.005
C2-H7	1.076	1.088	1.070	1.080	1.076
C3-H8	1.077	1.086	1.071	1.080	1.077

PM3 (Hyperchem8.0.6), ab initio and DFT (Gaussian09)

Table 2 Angles in degree of pyrrole molecule

Angle	Exp. ⁵¹	PM3	Ab initio /HF /6-31G(d,p)	DFT/B3LYP /6-31G(d,p)	Ab initio /MP2 /6-31G(d,p)
N1-C2-C3	107.70	107.04	108.18	107.70	107.41
C2-C3-C4	107.40	108.10	107.10	107.42	107.52
C2-N1-C5	109.80	109.72	109.44	109.77	110.14
C2-N1-H6	125.10	125.14	125.28	125.11	124.93
N1-C2-H7	121.50	123.66	121.18	121.12	121.23
C2-C3-H8	125.50	126.29	125.95	125.72	125.54

PM3 (Hyperchem8.0.6), Ab initio and DFT (Gaussian09)

Table 3. Net charge distribution for pyrrole molecule.

Pyrrole atoms	Ab initio/HF /6-31G(d,p)	DFT/B3LYP /6-31G(d,p)	Ab initio/MP2 /6-31G(d,p)
N1	-0.629	-0.485	-0.629
C2	0.078	0.070	0.069
C3	-0.212	-0.128	-0.208
C4	-0.212	-0.128	-0.208
C5	0.078	0.070	0.069

Ab initio and DFT (Gaussian09)

The molecular electrostatic potential MESP yields information on the molecular regions that are preferred or avoided by an electrophile or nucleophile. Any chemical system creates an electrostatic potential around it self. When a hypothetical

‘volumeless’ unit positive charge is used as a probe, it feels the attractive or repulsive forces in regions where the electrostatic potential is negative or positive respectively⁵².

It has been found to be a very useful tool in the investigation of the correlation between the molecular structure and the physiochemical property relationship of molecules including biomolecules and drugs⁵²⁻⁵⁶. The red and blue regions in the MESP map refer to regions of negative and positive potential and correspond to electron rich and electron-deficient regions respectively; where as the green color signifies neutral electrostatic potential⁵⁷.

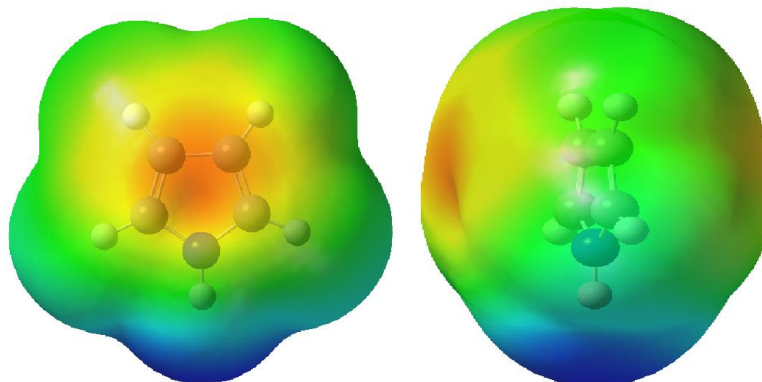


Fig.2 Two views of 3D MESP surface of pyrrole (GaussView 5)

The MESP surface map for pyrrole shows that the region near the carbon atoms is rich with electrons due to the red color that refer to a negative potential in the other hand the region between the carbon atoms and their hydrogens is yellow which indicate

a less negative potential than the previous one. The green regions refer to a neutral electrostatic potential, but the blue small region signifies a slight deficient in electrons compared to the major positive potential region around the hydrogen attached to the nitrogen atom, which is characterized by the dark blue color that indicate this regions bears the maximum brunt of positive charge.

3.2. *Electronic Structure of substituted pyrroles*

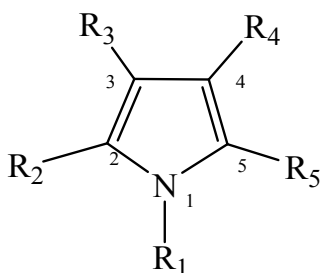


Fig. 3 Scheme of pyrrole systems.

1	$R_1 = R_2 = R_3 = R_4 = R_5 = H$
2	$R_2 = CH_3, R_1 = R_3 = R_4 = R_5 = H$
3	$R_3 = CH_3, R_1 = R_2 = R_4 = R_5 = H$
4	$R_2 = R_3 = CH_3, R_1 = R_4 = R_5 = H$
5	$R_2 = R_4 = CH_3, R_1 = R_3 = R_5 = H$
6	$R_2 = R_5 = CH_3, R_1 = R_3 = R_4 = H$
7	$R_3 = R_4 = CH_3, R_1 = R_2 = R_5 = H$
8	$R_2 = R_3 = R_4 = CH_3, R_1 = R_5 = H$
9	$R_2 = R_3 = R_5 = CH_3, R_1 = R_4 = H$
10	$R_2 = R_3 = R_4 = R_5 = CH_3, R_1 = H$

Calculated values of methyl substituted pyrroles (Figure 3) are given in Tables 4-5.

In the Table 4, heat of formation, dipole moment, HOMO (highest occupied molecular orbital), LUMO (lowest unoccupied molecular orbital) and their difference (ΔE) are

reported for pyrrole and its methyl derivatives. Net atomic charges are reported in the Table 5.

The heat of formation of studied compounds is varying from -11.277 Kcal/mol to 26.979 Kcal/mol. The compound 10 has the lowest heat of formation and needs small change in enthalpy to form one mole of this compound, while the compound 1 has the highest heat of formation and needs large change in enthalpy to form one mole of this compound.

It can be seen from the heat of formation data that approximately 10 kcal/mol is decreased at each addition of methyl group, in the base compound pyrrole irrespective of the number of substitutions.

The ionization potential values in compounds (1-10) shows a decreasing trend, which means increasing trend in the easy flow of charges in higher energy states of these compounds. The atomic charge of nitrogen slightly decreased in the methyl derivatives.

In the mono-substituted methyl group category, the 2-methyl pyrrole (compound 2) shows a maximum positive charge on the second position carbon (0.281), which leads

to a nucleophilic substitution and a maximum negative charge on the third carbon, which leads to an electrophilic substitution (Table5). This is further supported by the least HOMO-LUMO energy gap (0.226) as in Table 4, which depicts the chemical reactivity of the compound; the higher the HOMO-LUMO energy gap the lesser is the flow of electrons to the higher energy state making the molecule hard and less reactive. On the other hand, in lesser HOMO-LUMO gap, there is an easy flow of electrons to the higher energy state making it softer and more reactive (HSAB principle: hard and soft acids and bases). Hard bases have HOMO of low energy, and hard acids have LUMO of high energy⁵⁸. Compound 2 also shows a slightly high dipole moment value compared to the pyrrole molecule. C-H hyper-conjugation is the principal mode of electron release by the methyl group and leads to more stable excited states than the ground state.⁵⁹

In the case of dimethyl-substituted pyrroles, compound 6 presents the least HOMO-LUMO energy gap (0.2381) translating to better reactivity. Carbons C2 and C5 positions show a maximum negative charge (-0.158), which leads to preferential site of electrophilic attack the other hand the carbons C3 and C4 positions present a maximum

positive charge (0.283) which leads to preferential site of nucleophilic attack (Tables 4-5).

In the case of trimethyl-substituted pyrroles, compound 8 presents the least HOMO-LUMO energy gap (0.2347) translating to better reactivity. Carbon C4 positions show a maximum negative charge (-0.183), which leads to preferential site of electrophilic attack the other hand the carbon C5 positions present a maximum positive charge (0.286) which leads to preferential site of nucleophilic attack (Tables 4-5).

The 2,3,4,5-tetramethyl pyrrole (compound 10) is predicted to be the most reactive with the least HOMO-LUMO energy gap (0.2291) of all the pyrrole systems and the carbons C2 and C5 are the most preferential sites for nucleophilic attack with a net charge of (0.248). We found in literature that the majority of tetra-substituted pyrroles have biological activity.⁶⁰

We also note that the methyl substituent slightly increases the energy of HOMO with little change in decreasing the one of LUMO (Table 4).

Table 4. Energies of pyrrole and methyl-substituted pyrroles.

	Compound	ΔH_f (kcal/mol)	HOMO (au)	LUMO (au)	ΔE (au)	μ (Debye)
1	Pyrrole	26.9790	-0.2022	0.0495	0.2517	1.902
2	2-methyl pyrrole	16.8187	-0.1928	0.0492	0.2421	1.962
3	3-methyl pyrrole	17.6061	-0.1956	0.0488	0.2444	1.723

4	2,3-dimethy pyrrole	07.7076	-0.1871	0.0566	0.2437	1.829
5	2,4-dimethy pyrrole	07.5726	-0.1858	0.0524	0.2383	1.798
6	2,5-dimethy pyrrole	06.9264	-0.1817	0.0564	0.2381	1.992
7	3,4-dimethy pyrrole	08.4913	-0.1923	0.0521	0.2445	1.558
8	2,3,4-trimethyl pyrrole	-01.4929	-0.1837	0.0510	0.2347	1.638
9	2,3,5-trimethyl pyrrole	-02.4226	-0.1792	0.0556	0.2348	1.822
10	2,3,4,5-tetramethyl pyrrole	-11.2771	-0.1748	0.0543	0.2291	1.676

ΔH_f calculated by PM3 (Hyperchem8.0.6) HOMO, LUMO, ΔE , μ calculated by DFT (Gaussian 09)

Table 5. Net atomic charges for methyl-substituted pyrroles.

Compound	1	2	3	4	5	6	7	8	9	10
N	-0.485	-0.526	-0.493	-0.535	-0.538	-0.569	-0.501	-0.544	-0.579	-0.586
C2	0.070	0.281	0.038	0.245	0.287	0.283	0.037	0.248	0.250	0.248
C3	-0.128	-0.154	0.071	0.051	-0.180	-0.158	0.048	0.023	0.048	0.027
C4	-0.128	-0.133	-0.152	-0.154	0.072	-0.158	0.054	0.055	-0.183	0.027
C5	0.070	0.072	0.071	0.068	0.035	0.283	0.034	0.034	0.286	0.248
C-methyl-2	-	-0.380	-	-0.375	-0.375	-0.378	-	-0.381	-0.378	-0.376
C-methyl-3	-	-	-0.377	-0.379	-	-	-0.381	-0.383	-0.379	-0.381
C-methyl-4	-	-	-	-	-0.379	-	-0.379	-0.379	-	-0.384
C-methyl-5	-	-	-	-	-	-0.378	-	-	-0.382	-0.382

Net charge calculated by DFT (Gaussian09)

3.3. Study of Structure-Property/ Activity Relationships (SPR/SAR) for Pyrrole

Derivatives

Here we carry out the Structure Activity/Property Relationship (SAR/SPR) studies which are attempting to enhance our understanding of fundamental processes and phenomena in medicinal chemistry and drug design ⁶¹ and to give us the correlation between molecular structures and properties ⁶² such as lipophilicity, polarizability, electronic and steric

parameters. The molecular properties, used in the correlations, relate as directly as possible to the key physicochemical processes taking place in the target activity.

An important objective for this project was to evaluate the physicochemical domain of the some pyrrole derivatives (Fig.4) reported in literature has a biological activity⁶⁰. Some of physicochemical properties were calculated using HyperChem 8.03 software like (Surface Area, Volume, Polarizability, logP, Refractivity and Hydration Energy) and others were calculated using Molinspiration online database (TPSA and nrotb, hydrogen bond donor (HBD) and hydrogen bond acceptor (HBA)). We will continue this work in the future by a quantitative calculation.

Molecular volume determines transport characteristics of molecules, such as intestinal absorption or blood-brain barrier penetration. Volume is therefore often used in QSAR studies to model molecular properties and biological activity.

The molar refractivity is a steric parameter that is dependent on the spatial array of the aromatic ring in the synthesized compounds. The spatial arrangement also is necessary to study the interaction of the ligand with the receptor⁶³. Molecular refractivity is related, not only to the volume of the molecules but also to the London dispersive forces that act in the drug receptor interaction.

Molecular Polarizability of a molecule characterizes the capability of its electronic system to be distorted by the external field, and it plays an important role in modeling many molecular properties and biological activities ⁶⁴.

Solvent-accessible surface bounded molecular volume and van der Waals-surface-bounded molecular volume calculations are based on a grid method derived by Bodor et al. ⁶⁵, using the atomic radii of Gavezotti⁶⁶.

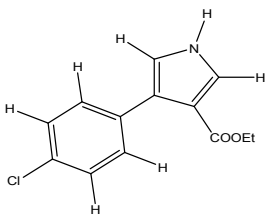
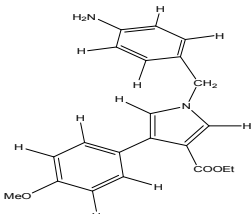
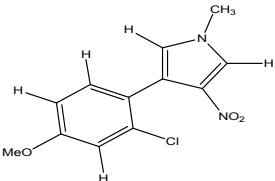
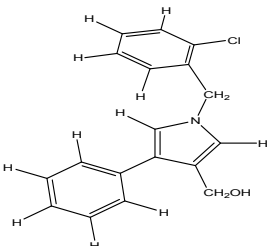
Hydration energy is a key factor determining the stability of different molecular conformations in water solutions ⁶⁷. The calculation is based on exposed surface area as computed by the approximate method (above), weighted by atom type. Total polar surface area (TPSA) is a very useful parameter for prediction of drug transport properties. Polar surface area is defined as a sum of surfaces of polar atoms (usually oxygens, nitrogens and attached hydrogens) in a molecule. This parameter has been shown to correlate very well with the human intestinal absorption, Caco-2 monolayer's permeability, and blood-brain barrier penetration ⁶⁸.

Molecules with TPSA values of 140 Å² or more are expected to exhibit poor intestinal absorption, TPSA was used to calculate the percentage of absorption (%ABS) according to the equation: $\%ABS = 109 \pm 0.345 \times TPSA$, as reported ⁶⁹. Number of rotatable bonds (nrotb) is a simple topological parameter that measures molecular flexibility and is considered to be a

good descriptor of oral bioavailability of drugs⁷⁰. Rotatable bond is defined as any single non-ring bond, bounded to non terminal heavy (i.e., non-hydrogen) atom. Amide C-N bonds are not considered because of their high rotational energy barrier.

3.3. 1. Structural comparison of pyrrole derivatives

Based on our conclusions on the effect of substitution on the pyrrole molecule, we chose a series of pyrrole derivatives (Antimycobacterial Pyrroles); these molecules possess a biological activity. The present series of pyrrole derivatives have been synthesized and characterized by Di Santo et al.⁷¹⁻⁷⁴. Initially, we performed a structural comparison of this series Figure 4. For example, Figure 5 shows the favored conformation in 3D of the compound 3.

N°	structure	N°	structure
1		7	
2		8	

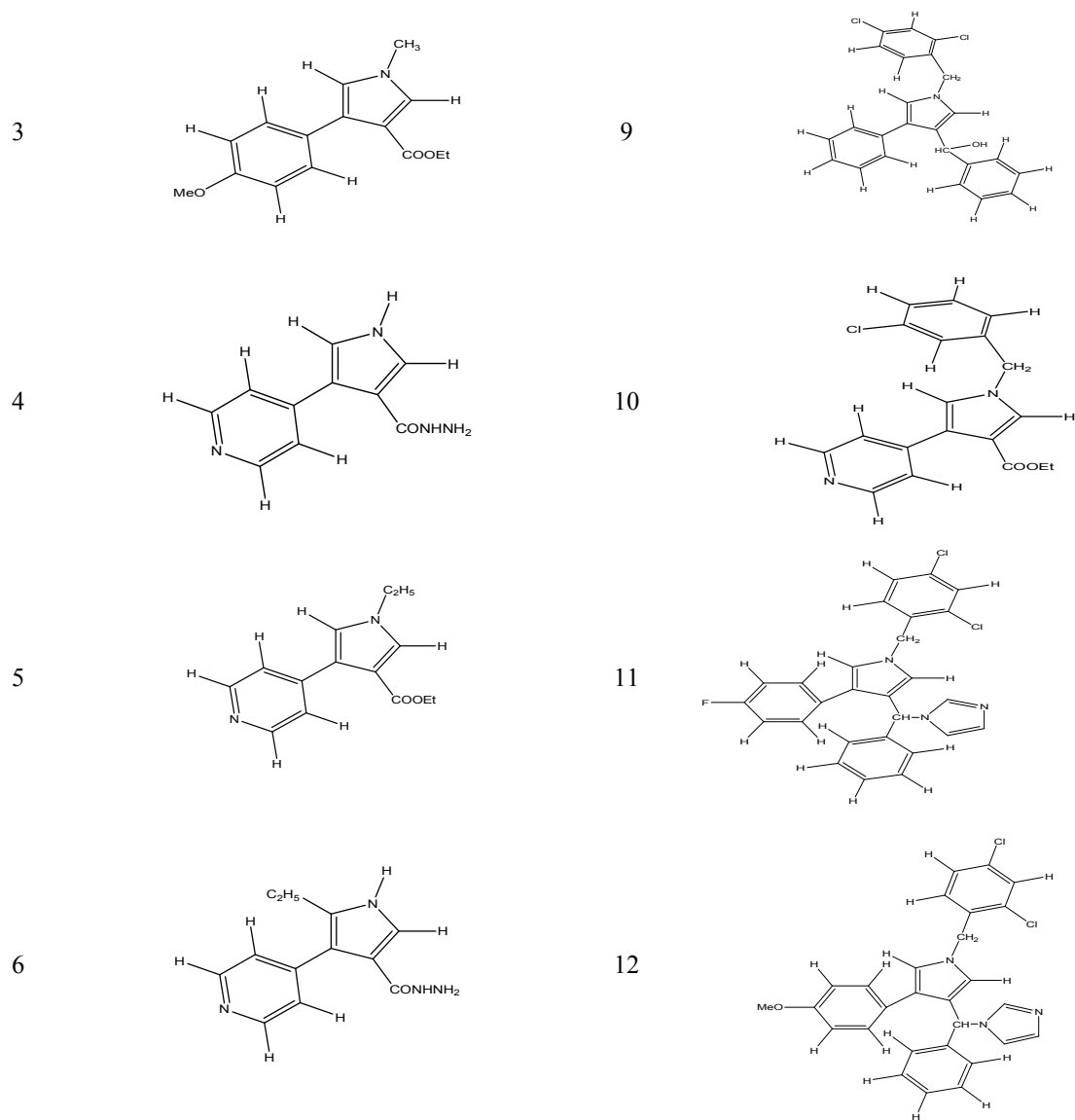


Fig. 4. Structural comparison of the pyrrrole derivatives

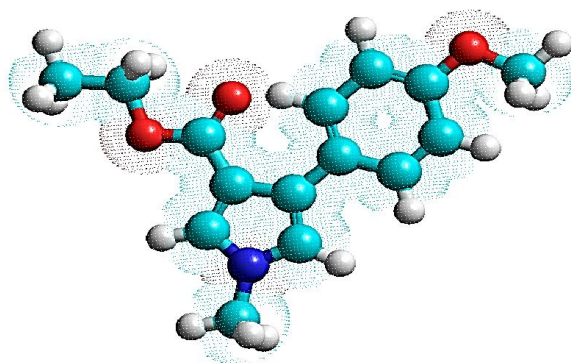


Fig. 5. 3D Conformation of compound 3 (HyperChem 8.03)

3.3. 2. Structure and physical-chemistry activity relationship

Polarizability values are generally proportional to the values of surfaces and of volumes, the decreasing order of polarizability for these studied pyrrole derivatives is: 12 > 11 > 9 > 7 > 10 > 8 > 3 > 5 > 2 > 1 > 6 > 4. [Table 6].

The order of polarizability is approximately the same one for volume and surface. This is also explained by the relation between polarizability and volume, for the relatively non polar molecules.

The polarizability of a molecule depends only on its volume; the thermal agitation of the non polar molecules does not have any influence on the appearance of dipole moments in these molecules. On the other hand for the polar molecules, the polarizability of the molecule does not depend solely on volume but also depends on other factors such as the temperature, because of the presence of the permanent dipole. For these pyrrole derivatives, surfaces vary from 373.484 to 694.037 Å². These pyrrole derivatives have a great variation of distribution volume, in particular compound 11 and compound 12 which have respective volumes: 1203.791 and 1276.280 Å³ [Table 6].

Hydration energy in absolute value, the most important is that of the compound 4 (-16.806 Kcal/mol) and the smallest value is that of the compound 5 (-2.997 kcal/mol). Indeed,

in the biological environments the polar molecules are surrounded by water molecules. They are established hydrogen bonds between them.

Hydrophobic groups in pyrrole derivatives induce a decrease of hydration energy, however, the presence of hydrophilic groups as in compound 4 (Fig. 6) possessing four (HBD) hydrogen bond donors (4NH) and five (HBA) hydrogen bond acceptors (4N, 1O), result the increase in the hydration energy. Otherwise, the compound 5 (Fig. 6) has the smallest value of hydration energy in absolute value (2.997) possessing only four (HBA) hydrogen bond acceptors (2N, 2O), which result in decreasing the hydration energy.

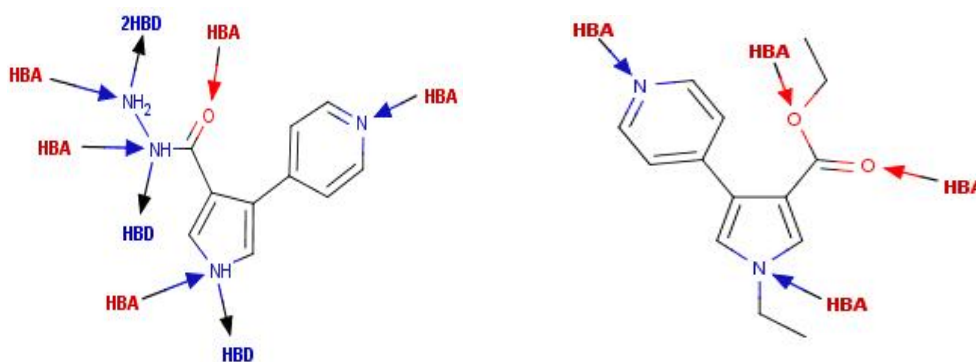


Fig. 6. Donor and acceptor sites of compound 4 and 5.

We can be observed obviously that all the title compounds (1–12) exhibited a great %ABS ranging from 80.08 - 100.32%, indicating that these compounds should have good cellular plasmatic membrane permeability [Table 6]. Most of the compounds also showed a PSA of less than 140 \AA^2 , all the screened compounds were flexible, especially, compounds 7 and 12 which have 7 rotatable bonds, and rotatable Bond Countless than 10 [Table 6].

Table 6. QSAR proprieties for pyrrole derivatives

Compound	SAG	Vol	HE	LogP	Ref	Pol	TPSA	nrotb	ABS%
1	447.308	722.341	-5.538	-0.261	71.527	26.123	42.10	4	94.476
2	442.938	716.173	-11.446	-4.935	73.332	26.498	59.99	3	88.303
3	488.845	798.050	-3.715	-0.785	78.082	28.502	40.47	5	95.038
4	373.484	583.647	-16.806	-2.763	60.031	21.881	83.80	2	80.089
5	469.829	760.482	-2.997	-0.922	72.886	27.156	44.13	5	93.775
6	419.068	676.070	-14.634	-2.267	70.342	25.551	83.80	3	80.089
7	603.681	997.873	-5.227	0.228	106.834	38.162	40.47	7	95.038
8	518.218	855.928	-5.715	0.391	95.716	33.862	25.16	4	100.320
9	627.778	1081.896	-6.548	1.253	128.853	45.450	25.16	5	100.320
10	580.319	960.294	-4.753	-0.474	101.606	36.909	44.13	6	93.775
11	680.890	1203.791	-5.234	0.192	145.628	51.546	44.13	6	101.148
12	694.037	1276.280	-6.714	-0.200	151.875	54.109	31.99	7	97.963

3.3. 3. Drug likeness calculation on the basis of Lipinski rule of five

Structures of all the selected pyrrole derivatives (fig. 4) were drawn by using ACD labs ChemsSketch v 12.0⁷⁵ and their SMILES notations were generated. Smiles notations of the selected compounds were fed in the online Molinspiration software version (www.molinspiration.com) for calculation of molecular properties (number of hydrogen bond donors and acceptors, molecular weight). Drug-likeness appears as a promising paradigm to encode the balance among the molecular properties of a compound that influences its pharmacodynamics and pharmacokinetics and ultimately optimizes their absorption, distribution, metabolism and excretion (ADME) in human body like a drug⁷⁶. These parameters allow to ascertaining oral absorption or membrane permeability that occurs when

the evaluated molecule follows Lipinski's rule of five [molecular weight (MW) \leq 500 Da, $\log P \leq 5$, H-bond donors (HBD) ≤ 5 and H-bond acceptors (HBA) ≤ 10]. Molecules violating more than one of these parameters may have problems with bioavailability and high probability of failure to display druglikeness^{77, 78}.

However, there are some exceptions to this rule and a compound is likely to be orally active as long as it did not break more than one of his rules because some of orally active drugs such as atorvastatin, cyclosporine do not obey the rule of five.

Octanol/water partition coefficient (LogP) are widely used to make estimation for membrane penetration and permeability, including gastrointestinal absorption^{79,80}, blood-brain barrier (BBB) crossing,^{81,82} and correlations to pharmacokinetic properties⁸³.

Log P values of pyrrole derivatives, were found to be in the range of -4.93 to 1.25.

Compound 2 is expected to have the highest hydrophilicity because its log P value, whereas compound number 9 will be the most lipophilic. This implies that these compounds will have poor permeability across cell membrane. Some structural modifications should be carried out to improve their oral absorption, bioavailability and permeability.

Low molecular weight drug molecules (<500) are easily transported, diffuse and absorbed as compared to heavy molecules.

Number of hydrogen bond acceptors (O and N atoms) and number of hydrogen bond donors (NH and OH). These quantities had shown to be critical in a drug development setting as they influence absorption and permeation⁸⁴. In the tested compounds were found to be within Lipinski's limit i.e. less than 10 and 5 respectively.

The calculation results show that all compounds meet the Lipinski rules of the five, suggesting that these compounds theoretically would not have problems with oral bioavailability.

Table 7. Lipinski's rule of five for drug likeliness of pyrrole derivatives

Compound	mass	nOH, NH	nO, N	logP	n violations
1	249.697	1	3	-0.261	0
2	267.692	0	5	-4.935	0
3	259.305	0	1	-0.785	0
4	202.216	4	5	-2.763	0
5	244.293	0	4	-0.922	0
6	230.269	4	5	-2.267	0
7	335.403	0	4	0.228	0
8	297.784	1	2	0.391	0
9	408.327	1	2	1.253	0
10	340.809	0	4	-0.474	0
11	476.380	0	4	0.192	0
12	488.416	0	4	-0.200	0

4. CONCLUSIONS

The present study provides a discussion of several molecular properties of pyrrole and its derivatives, based on Ab initio and density functional theory calculations. The method DFT at the level of B3LYP with 6-31G(d,p) basis; shows a good agreement with experimental data.

This method can be used quite satisfactorily in predicting the chemical reactivity of the molecules and the effect of substitution of either donor electron. The application of Lipinski rules on the studied pyrrole derivatives shows that the studied compounds, theoretically will not have any problems with oral bioavailability.

5. REFERENCES

- [1] E.Toja , A. Depaoli , G.Tuan, J. Kettenring, *Synthesis*, 272, 274(1987).
- [2] M. Joseph, H. M. Stefan, T. Unger, J. Ackrell, P. Cheung, F.Gary, C.J.Cook, *J.Med. Chem.*, 28,1037 (1985).
- [3] G. Dannhardt, W.Kiefer, G. Kramer, S. Maehrlein, U. Nowe, B. Fiebich, *Eur. J. Med .Chem.*, 35, 499(2000).
- [4] J.T. Gupton, B.S. Burnham, B.D. Byrd, K.E. Krumpe, C. Stokes, J. Shuford , S.Winkle,T.Webb, A.E. Warren, C, Barnes, J. Henry, I.H. Hall, *Pharmazie*, 54, 691(1999).
- [5] M.H. Justin, K. O'Toole-Colin, A. Getzel, A. Argenti, A. Michael, *Molecules*,2004, 9,135(2004).
- [6] K. Krowicki, T. Jan Balzarini, Erik de Clercq , A.Robert, Newman, J. WilliamLawn, *J.Med.Chem.*,31,341(1988).
- [7] A.M. Almerico, P. Diana, P.Barraja, G. Dattolo, F. Mingoia, A.G. Loi, F. Scintu, C.Milia,I. Puddu,P. La Colla, *Farmaco.*, 53,33(1998).
- [8] H.Carpio, E. Galeazzi, R. Greenhouse, A. Guzman, E. Velarde, Y. Antonio, *Can. J. Chem.*, 60, 2295(1982).
- [9] D.T.Dannhar, G. Kiefer, W. Kramer, G. Maehrlein, S. Nowe, U. Fiebich, *Eur. J. Med.Chem.*, 35, 499(2000).
- [10] M.A. Evans, D.C. Smith, J.M. Holub, A. Argenti, M. Hoff, G.A. Dalglish, *Arch.Pharm.Pharm. Med. Chem.*,336, 181(2003).
- [11] D. Harkati, S. Belaidi, A. Kerassa, and N. Gherraf , *Quantum Matter*, 5, 36-44 (2016)
- [12] A. Kerassa, S. Belaidi and T. Lanez, *Quantum Matter*,5, 45-52 (2016)

- [13] Z. Almi, S. Belaidi, N. Melkemi, S. Boughdiri and L. Belkhiri , *Quantum Matter*, 5, 124-129 (2016)
- [14] M. Mellaoui, S. Belaidi, D. Bouzidi, and N. Gherraf, *Quantum Matter*, 3, 435-441 (2014)
- [15] W.J. Hehre, *Practical Strategies for Electronic Structure Calculations*, Wave functions", Inc., Irvine, California (1995).
- [16] C. M. Chang, H. L. Tseng, A. F. Jalbout, and A. de Leon, *J. Comput. Theor. Nanosci*, 10, 527, (2013).
- [17] T. L. Jensen, J. Moxnes, and E. Unneberg, *J. Comput. Theor. Nanosci*, 10, 464 (2013).
- [18] M. Narayanan and A. John Peter, *Quantum Matter*, 1, 53, (2012).
- [19] G. H. Coccoletzi and N. Takeuchi *Quantum Matter*, 2, 382-387 (2013).
- [20] S. Belaidi, A. Kerassa, T. Lanez, and M. Cinar , *J. Comput. Theor. Nanosci*. 12 (9), (2015), in press
- [21] S. Belaidi, H. Belaidi, and D. Bouzidi, *J. Comput. Theor. Nanosci*. 12, 1737-1745 (2015)
- [22] S. Belaidi, Z. Almi, and D. Bouzidi, *J. Comput. Theor. Nanosci*. 11, 2481-2488 (2014)
- [23] E. R. Davidson, *Chemical Reviews*, 91, 649 (1991).
- [24] H. Langueur, K. Kassali, and N. Lebga, *J. Comput. Theor. Nanosci*, 10, 86 (2013).
- [25] N. Melkemi and S. Belaidi, *J. Comput. Theor. Nanosci*, 11, 801 (2014).
- [26] M. Narayanan and A. John Peter, *Quantum Matter*, 1, 53 (2012).
- [27] Y. C. Martin, *Quantitative Drug Design*, Marcel Dekker, New York, NY, USA, (1978).
- [28] A.I. Ageenko and Y.E. Vitorgan, *Vopr. Virusol*, 2, 1599 (1975).
- [29] V.R. Talageri, S.N. Revankar, B.N. Mashelkar and K.I. Ranadive, *Biochem. Biophys*, 8, 79 (1971).
- [30] F.B. Hershey, G. Johnson, S.M. Murphy and M. Schmidt, *Cancer Res*, 26, 265 (1966).
- [31] T.T. Otani and H.P. Morris, *J. Natl. Cancer Inst. (US)*, 47, 1247 (1971).
- [32] J. G. Topliss, *Perspect. Drug Discov. Des*, 1, 253 (1993).
- [33] Zhigao Wang, Fangqiang Wang, Changhua Su, and Yongling Zhang *J. Comput. Theor. Nanosci*. 10, 2323-2327 (2013).
- [34] A. Eghdami and M. Monajjemi , *Quantum Matter*, 2, 324-331 (2013).
- [35] Yong Chen, Di Xu, and Min Yang, *J. Comput. Theor. Nanosci*. 10, 2916-2919 (2013).
- [36] A. Kerassa, S. Belaidi, D. Harkati, T. Lanez , O. Prasad, and L. Sinha , *Rev. Theor. Sci.*, 4, (2015) , in press

- [37] T. Salah, S. Belaidi, N. Melkemi, and N. Tchouar , *Rev. Theor. Sci.*, 3, 355-364 (2015)
- [38] Z. Almi, S. Belaidi, and L. Segueni, *Rev. Theor. Sci.* , 3, 264-272 (2015)
- [39] Q. Zhao, *Rev. Theor. Sci.* 1, 83-101 (2013).
- [40] A. Khrennikov, *Rev. Theor. Sci.* 1, 34-57 (2013).
- [41] N. Paitya and K. P. Ghatak, *Rev. Theor. Sci.* 1, 165-305 (2013).
- [42] E. L. Pankratov and E. A. Bulaeva, *Rev. Theor. Sci.* 1, 58-82 (2013).
- [43] M. Ibrahim and H. Elhaes, *Rev. Theor. Sci.* 1, 368-376 (2013).
- [44] J. Mazumder, R. Chakraborty, S. Sen, S. Vadra, B. De and T. K. Ravi, *Der Pharma Chemica*, 1(2), 188-198 (2009).
- [45] C. A. Lipinski, F. Lombardo, B. W. Dominy and P. J. Feeney, *Adv. Drug Deliv. Rev.* 4, 17 (2012).
- [46] HyperChem (Molecular Modeling System) Hypercube, Inc., 1115 NW, 4th Street, Gainesville, FL 32601; USA (2007). <http://www.hyperchem.com>.
- [47] Gaussian 09, Revision B.01, M. J. Frisch, G. W. Trucks, H. B. Schlegel, G. E. Scuseria, M. A. Robb, J. R. Cheeseman, G. Scalmani, V. Barone, B. Mennucci, G. A. Petersson, H. Nakatsuji, M. Caricato, X. Li, H. P. Hratchian, A. F. Izmaylov, J. Bloino, G. Zheng, J. L. Sonnenberg, M. Hada, M. Ehara, K. Toyota, R. Fukuda, J. Hasegawa, M. Ishida, T. Nakajima, Y. Honda, O. Kitao, H. Nakai, T. Vreven, J. A. Montgomery, Jr., J. E. Peralta, F. Ogliaro, M. Bearpark, J. J. Heyd, E. Brothers, K. N. Kudin, V. N. Staroverov, T. Keith, R. Kobayashi, J. Normand, K. Raghavachari, A. Rendell, J. C. Burant, S. S. Iyengar, J. Tomasi, M. Cossi, N. Rega, J. M. Millam, M. Klene, J. E. Knox, J. B. Cross, V. Bakken, C. Adamo, J. Jaramillo, R. Gomperts, R. E. Stratmann, O. Yazyev, A. J. Austin, R. Cammi, C. Pomelli, J. W. Ochterski, R. L. Martin, K. Morokuma, V. G. Zakrzewski, G. A. Voth, P. Salvador, J. J. Dannenberg, S. Dapprich, A. D. Daniels, O. Farkas, J. B. Foresman, J. V. Ortiz, J. Cioslowski and D. J. Fox, Gaussian, Inc., Wallingford CT, (2010).
- [48] Database, [<http://www.molinspiration.com>].
- [49] M. W. Wong, K. B. Wilberg and M. J. Frisch, *J. Am. Chem. Soc.*, 114, 1645 (1992).
- [50] V. Barone and C. Adamo, *J. Phys. Chem.* 99, 15062 (1995).
- [51] L. Nygaard, J. T. Nielsen, J. Kirchheiner, G. Maltesen, J. Rastrup-Andersen, G. O. Sorensen, *J. Mol. Struct.* 3, 491 (1969).

- [52] J. S. Murray & K. Sen, *Molecular Electrostatic Potentials, Concepts and Applications*. Elsevier, Amsterdam, (1996).
- [53] Alkorta, I. & J.J. Perez. *Int. J. Quant. Chem.* 57, 123–135 (1996).
- [54] Scrocco, E. & Tomasi, J. *Advances in Quantum Chemistry*, Academic Press. P. Lowdin (Ed.) New York (1978).
- [55] F. J. Luque, M. Orozco, P. K. Bhadane & S. R. J. Gadre, *Phys. Chem.* 97, 9380–9384 (1993).
- [56] J. Spöner & P. Hobza, *Int. J. Quant. Chem.* 57, 959–970 (1996).
- [57] S. R. Kumar, N. Vijay, K. Amarendra, P. Onkar & S. Leena, *Research Journal of Recent Sciences* 1, 11-18 (2012)
- [58] G.L. Miessler and D.A. Tarr, *Inorganic Chemistry, 2nd ed. Prentice-Hall*, New Jersey, USA, 181 (1999).
- [59] A. Weissberger, *the Chemistry of Heterocyclic Compounds*, John Wiley & Sons, New York, (1993).
- [60] R. Ragno, G. R. Marshall, R. Di Santo, R. Costi, S. Massa, R. Rompeiani, M. Artico, *Bioorg. Med. Chem.* 8, 1423–1432 (2000)
- [61] Z. Wang, F. Wang, C. Su, and Y. Zhang, *J. Comput. Theor. Nanosci.* 10, 2323 (2013).
- [62] G. Thomas, *Rev. Theor. Sci.* 2, 289 (2014).
- [63] P. Pankaj, C. R. Kapupara, A. S. Matholiya and R. D. Tusharbindu. *Inter. Int. bull. Drug. res.* 1(1), 1-10 (2011).
- [64] J. Wang, X. Q. Xie, T. Hou and X. Xu. *Fast. J. Phys. Chem. A.* , 111, 4443-4448 (2007).
- [65] N. Bodor, Z. Gabanyi, and C. Wong, *J. Am. Chem. Soc.* 111, 3783 (1989).
- [66] A. Gavezotti, *J. Am. Chem. Soc.* 100, 5220 (1983).
- [67] T. Ooi, M. Oobatake, G. Nemethy and H. A. Scheraga, *Proc. Natl. Acad. Sci. USA*, 84, 3086 (1987).
- [68] P. Ertl, B. Rohde, P. Selzer, *J. Med. Chem.* 43, 3714-3717 (2000).
- [69] V. N. Viswanadhan, A. K. Ghose, G. R. Revankar and R. K. Robins. *J. Chem. Inf. Comput.* 29, 163-172 (1989).
- [70] D. F. Veber, S. R. Johnson, H.Y. Cheng, B. R. Smith, K. W. Ward and K. D. Kopple. *J. Med. Chem.* 45, 2615-2623 (2002).
- [71] R. Di Santo, R. Costi, M. Artico, S. Massa, G. Lampis, D. Deidda, R. Pompei, *Bioorg. Med. Chem. Lett.* 8, 2931 (1998).

- [72] S. Massa, R. Di Santo, A. Mai, M. Botta, M. Artico, S. Panico, G. Simonetti, *Farmaco*. 45, 833 (1990).
- [73] S. Massa, R. Di Santo, R. Costi, A. Mai, M. Artico, A. Retico, G. Apuzzo, M. Artico, G. Simonetti, *Med. Chem. Research* 3, 192 (1993).
- [74] S. Massa, R. Di Santo, M. Artico, R. Costi, C. Di Filippo, G. Simonetti, A. Retico, M. Artico, *Eur. Bull. Drug Research* 1, 12(1992).
- [75]http://www.acdlabs.com/products/draw_nom/draw/chemsketch/
- [76]G. Vistoli, A. Pedretti and B. Testa, *Drug Discov Today*, (7-8), 285-294 (2008).
- [77]C. A. Lipinski, F. Lombardo, B. W. Dominy and P. J. Feeny. *Adv. Drug. Deliv. Rev.* 23, 3-25 (1997).
- [78] L. F. Supercomputing Facility for Bioinformatics & Computational Biology-IIT Delhi.L. *F.Available from: <http://www.scfbio-iitd.res.in>,*
- [79]S. Winiwarter, N. M. Bonham, F. Ax, A. Hallberg, H. Lennerna and A. Karlen. *J. Med. Chem.* 41, 4939–4949 (1998).
- [80]P. Artursson and J. Karlsson, *Biochem. Biophys. Res. Commun.* 175, 880–885 (1991).
- [81]R. C. Young, R. C. Mitchell, T. H. Brown, Ganellin, R. Griffiths, M. Jones, K. K. Rana, D. Saunders, I. R. Smith, N. E. Sore and T. J. Wilks. *J. Med. Chem.* 31, 656–671 (1988).
- [82] H. V. d. Waterbeemd, G. Camenisch, G. Folkers, J. R. Chretien and O. A. Raevsky. *J. Drug. Target.* 2, 151–165 (1998).
- [83]D. A. Smith, B. C. Jones and D. K. Walker. *Med. Res. Rev.* 16, 243–266 (1996).
- [84]G. W. Bemis and M. A. Murcko. *J. Med. Chem.* 39, 2887-2993 (1996).

CHAPITRE IV:

**Vibronic Coupling to Simulate the
Phosphorescence Spectra of Ir(III) Based
OLED Systems: TD-DFT Results Meet
Experimental Data**

1. Introduction

In the past decades, transition metal complexes have been extensively studied, especially particularly thanks to their strong ability to luminescence. Furthermore, compounds demonstrating a high emission response to stimuli are of interest for the development of organic light-emitting diodes (OLED) systems or light-emitting cells (LEC).[1–3] Among them, one can cite iridium complexes which possess this strong ability to emit in large energetic range.[4–10] Furthermore, iridium, ruthenium or platinum complexes are among the most investigated compounds and numerous studies from both the experimental and computational sides have been reported due to their strong ability to be embedded in devices.[4, 5, 8–17]

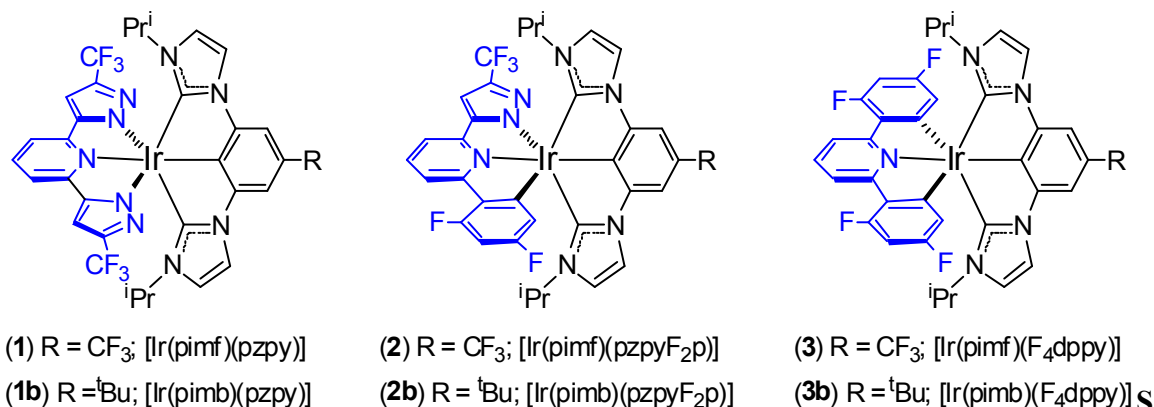
From an experimental point view, it remains challenging and difficult to fully characterize the electronic processes at work within the targeted compounds. As a matter of facts, chemists from quantum chemical computations are now able to give crucial information on these electronic processes, namely the excitation and emission phenomena and the nature of the reached excited states, especially thanks to the very recent developments in this area.[18–23] Moreover, Density Functional Theory (DFT) and its time dependent extension (TD-DFT) are now routinely used to get both electronic and vibrational information from small organic to large-size organometallic and transition metal complexes systems:[10, 24–30] Indeed, DFT calculations are now accurate enough to predict or confirm the stability or existence of compounds, and they can also explain the luminescent and/or spectroscopic properties of multi-scale systems. [31–40]

In the field of spectroscopy calculations, Vlcek Jr. and Zális among other authors, have shown how DFT and TD-DFT are useful tools to study d^6 metal complexes.[41]

The computation of the vibrational structure of electronic absorption or emission bands should permit to reproduce more accurately both the position and the band shape of the observed spectra

. In this context, Barone and coworkers implemented recently the so called Virtual Multifrequency Spectrometer (VMS)[42, 43] which is a powerful, mature and cheap tool to simulate many types of spectroscopy, even when one wishes to investigate large systems or a large number of effects (solvent, anharmonicity and Duschinsky couplings) in order to simulate more accurately the spectra.[50–59] Indeed, in the last years, the VMS approach has been used to simulate with high precision anharmonic and phosphorescence spectra of organometallics and transition metal complexes. [9, 18, 21–23]

New tridentate chelate Ir(III) complexes have been very recently synthesized and characterized by Chi and co-workers [personal communication]. These neutral complexes (Scheme 1) involving *bis*(imidazolylidene) benzene and 2-(5-trifluoromethyl-1H-pyrazol-3-yl)-6-(2,4-difluorophenyl) pyridine (pzpyF₂p) or 2,6-bis(5-trifluoromethylpyrazol-3-yl) pyridine (pz₂py) ligands, exhibit a blue-shifted phosphorescence very suitable for OLED devices. Interestingly, it is observed that complex **1** does not phosphor in solution, contrarily to complexes **2** and **3**, but all complexes emit when suitably processed as films. Moreover, whereas complexes **2** and **2b** exhibit a structured emission band, it is not the case for complexes **3** and **3b** which exhibit a structure less phosphorescence band. In this paper, we report a full quantum investigation based on DFT and TD-DFT methods of these Ir(III) complexes in order to explain the observed properties and to help to the design of complexes of such technological interest. We first discuss the ground state (GS) characteristics, *i.e.* the geometric and electronic structures. In a second step we focus our attention on the optical properties. We shall propose an assignment of the observed absorption band using TD-DFT. Then, the lowest triplet excited state (ES) will be studied. The combinations of these computations together with the aforementioned powerful tools, namely taking into account vibronic couplings, should permit to rationalize the observed properties.



cheme 1. Investigated bis-tridentate Ir(III) complexes.

2. Computational details

All calculations have been performed at the DFT level of theory employing the G09 suite of programs.[59] On the basis of several previous studies,[9, 10, 22]we have chosen the B3PW91 functional to perform the computations.[60–62]The associated basis set is the so-called LANL2DZ one, including a pseudo potential for inner electrons of Ir and augmented with polarization functions on C(d; exponent 0.587), N(d; 0.736), F(d; 1.577) Ir(f; 0.938).[63–66]Solvent effects (CH₂Cl₂) have been taken into account by the Polarizable Continuum Model (PCM).[67, 68]All the GS geometries have been optimized and checked to be true minima on the Potential Energy Surface (PES) by diagonalizing their Hessians. Grimme’s corrections for dispersion with Becke-Johnson damping (GD3BJ) have been also included in the computations.[69] Time-Dependent Density Functional Theory (TD-DFT) computations have been performed, using the optimized ground state geometries, to obtain excitations energies and spectra. Then, in order to plot the phosphorescence spectra, vibronic contributions to electronic emission have been considered using the Adiabatic Shift (AS) approach as implemented in the used version of the Gaussian Package.[42, 70] In the case of complex **3**, some normal modes

have been removed of the vibronic treatment in order to reach a sufficient spectrum convergence. Orbital visualization has been done using the GaussView[71] program and the orbital composition has been obtained using the AOMix package.[72]The simulated UV-visible and phosphorescence spectra have been respectively plotted using the Swizard[73] and the VMS programs.[43]

3. Results and discussion

3.1. Ground state geometric structures

The optimized geometries are compared with the experimental data (Table 1 and ESI). In this section the discussion of the geometry is focused on complex **1** but the trend is the same for the other compounds.

Table 1. Selected experimental and computed parametric data of complex **1**.

Bond lengths (Å)	Ir-C	Ir-N	
X-ray	1.965(5)	2.046(3)	
	2.078(5)	2.052(4)	
	2.056(4)	2.038(4)	
DFT	1.969	2.028	
	2.039	2.047	
	2.040	2.031	
Angles (°)	C-Ir-C	N-Ir-N	C-Ir-N
X-ray	154.9(18)	155.6(15)	178.7(18)
DFT	155.7	156.9	179.5

In average the computed M-L bond lengths fit nicely the observed ones, even if a slight underestimation in the simulation is observed. The angles around the metal are also well reproduced in our calculations with a deviation of less than 1° in comparison to the X-ray data. This trend also matches what some of us have reported before, *i. e.* the methodology

(B3PW91/LANL2DZ+pol.) provides very accurate geometries in the simulations with respect to X-ray experiments.[9, 10]

3.2. Ground state electronic structures and electronic vertical excitations

We now focus our attention on the electronic structures. On the optimized GS geometries, TD-DFT vertical excitations computations have been performed. The charge transfers occurring during excitations for the six complexes are described thanks to their electronic structures. As the *PimF* and *PimB* ligands differ only by a CF₃ replaced by a ^tBu group on the benzene ring, the properties of their related complexes (*e.g.* **1**, **1b**) are relatively similar; therefore the discussion will be mainly focused on complexes **1**, **2** and **3**. Furthermore, as we found that the frontier orbitals are similar for all complexes, only the molecular orbital (MO) diagram of **1** is discussed (Figure 1). The highest occupied molecular orbitals are mainly localized on the metal atom (*d* orbitals) whereas the lowest unoccupied orbitals are π^* types localized on the ligands. (**1b**, **2b** and **3b** MO diagrams are in ESI). One should mention that, as expected, the CF₃ moieties are not involved in the frontier orbitals.

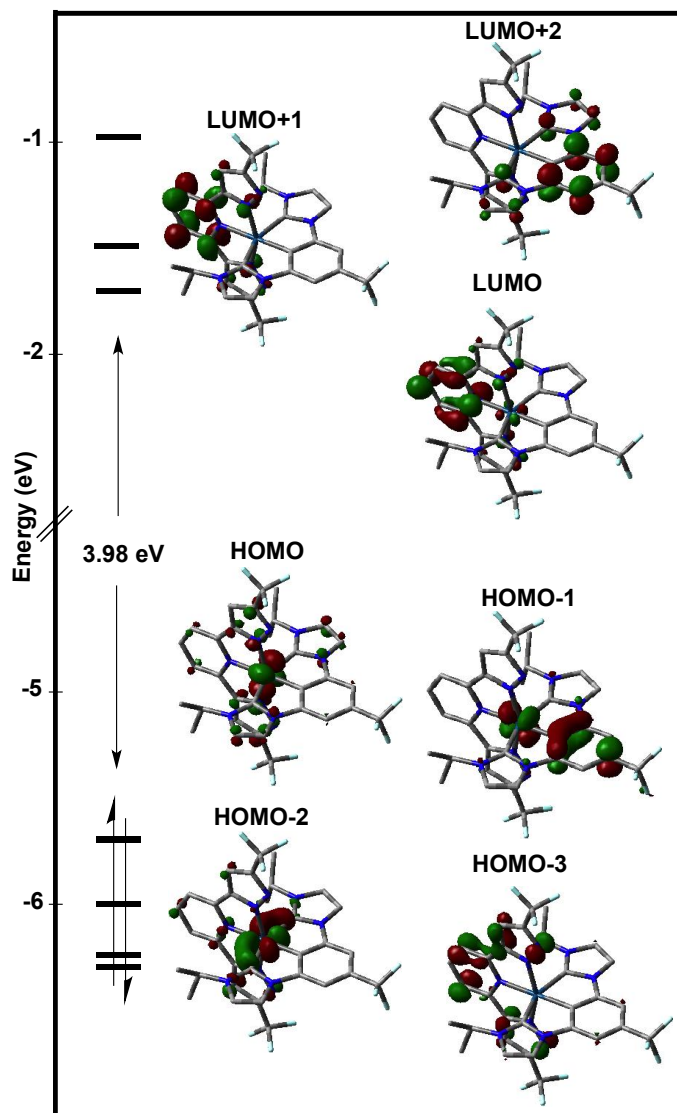


Figure 1. Frontier orbitals diagram of complex 1.

Using these optimized geometries, TD-DFT calculations have been performed to simulate the electronic absorption spectra based on the vertical excitations, and compared to the experimental ones (Figure 2). The observed and simulated absorption spectra are in good agreement; both the computed transition energies and intensities fit nicely the experimental data. Furthermore, the observed absorption red shift between complexes from **1** to **3** is also well reproduced in the

simulations. It turned out that the modulation of the ligand also tuned the absorption bands. Indeed it is observed a small red shift when *PimB* ligand is used instead of *PimF*. This trend is also well portrayed in the simulations. The discussion is now focused on the band assignment. In Table 2 and Table 3 are provided the experimental and calculated electronic transitions (f is the oscillator strength of the excitation). In order to assign the transition bands, the MOs compositions are collected in Table S1. All complexes exhibit a very weak absorption band around 400 nm and an intense one between 315 and 345 nm.

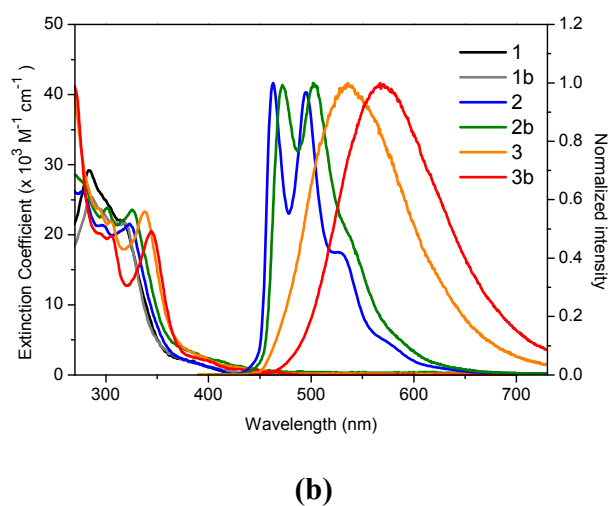
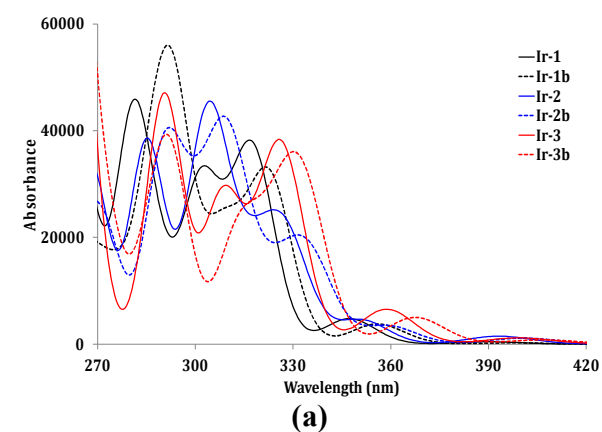


Figure 2. Simulated Electronic Absorption Spectra (a). Observed Absorption and Luminescence Spectra (b).

Table 2. Experimental and calculated vertical excitations maxima.

Cplx	$\lambda_{\text{Exp}}/\text{nm}$ (ϵ) ^a	$\lambda_{\text{Calc}}/\text{nm}$ (f) ^b	$\lambda_{\text{max}}/\text{nm}$
1	316 (21.9)	317 (0.204)	317
	406 (0.8)	320 (0.033)	390
		390 (0.003)	
1b	318 (21.7)	309 (0.146)	318
	409 (0.9)	322(0.204)	397
		397 (0.002)	
2	323 (21.6)	318 (0.079)	324
	407 (0.9)	328 (0.130)	393
		393 (0.010)	
2b	325 (23.5)	324 (0.072)	329
	418 (1.7)	334 (0.111)	400
		401 (0.007)	
3	338 (23.3)	325 (0.070)	326
	431 (0.9)	327 (0.183)	399
		399 (0.008)	
3b	345 (20.4)	332 (0.309)	333
	433 (0.7)	333 (0.156)	407
		407(0.005)	

^a10⁻³ M⁻¹ cm⁻¹^b Oscillator strengths

Based on results given in Table 3, one should see that for complexes **1** and **2** the lowest energy excitations correspond to HOMO → LUMO transitions. It corresponds to a Metal to Ligand Charge Transfer (MLCT). A similar trend is observed for other excitations despite that the HOMO-3, which is localized on the π orbitals of the pyridine ligand, becomes involved for transitions at higher energy. This result can be of importance to explain the absence of luminescence, especially for complex **1**. Indeed, it turns out that the highest energy excitations reported for complex **1** is mainly a HOMO-3 to LUMO+1(82%) transition, whereas for complex **2** it is an admixture of two excitations with a weak involvement of this particular transition (27%).

Table 3. Band assignments of complexes **1** and **2**.

1		
$\lambda_{\text{Calc}}(\text{nm})$	f	Transitions
390	0.003	HOMO \square LUMO (98%)
347	0.033	HOMO \square LUMO+1 (89%)
320	0.033	HOMO-3 \square LUMO (52%)
		HOMO-2 \square LUMO+1 (39%)
317	0.204	HOMO-2 \square LUMO (72%)
302	0.209	HOMO-2 \square LUMO+1 (54%)
		HOMO-3 \square LUMO (42%)
280	0.239	HOMO-3 \square LUMO+1 (82%)
2		
393	0.010	HOMO \rightarrow LUMO (95%)
351	0.031	HOMO \rightarrow LUMO+1 (86%)
		HOMO-2 \rightarrow LUMO (10%)
328	0.130	HOMO-2 \rightarrow LUMO (74%)
318	0.079	HOMO-3 \rightarrow LUMO (50%)
		HOMO-2 \rightarrow LUMO+1 (31%)
305	0.230	HOMO-2 \rightarrow LUMO+1 (56%)
		HOMO-3 \rightarrow LUMO (36%)
285	0.217	HOMO-1 \rightarrow LUMO+3 (44%)
		HOMO-3 \rightarrow LUMO+1 (27%)

3.3. Luminescence properties

Experimentally, contrarily to complexes **2** and **3**, complex **1** did not exhibit luminescence signature, in solution but only when processed as a film [to be published]. Several hypotheses arise from the analyses of MOs compositions and from the band assignments. Indeed, as exposed above, the lowest absorption wavelength is mainly centred on ligands for complex **1**, whereas for complex **2** the HOMO-1 is the most involved and is localized on the metal. Another hypothesis comes from the fact that there is an unoccupied orbital, low in energy, localized on the metal for complex **1** (LUMO +7). Thus, it is probable that a non-emissive 3 MC state could be reached via the 3 MLCT one for complex **1**. Moreover, the computed oscillator strength of the MLCT band around 400 nm, is very low in solution for complex **1** compared to the other complexes, knowing that 400 nm is the used excitation wavelength for emission. Adding these two factors is likely to explain the quenching of its emission in solution. Complexes **2** and **3** exhibit interesting and

different luminescence properties. Indeed complex **2** shows a structured emission band whereas complex **3** possesses a single band. In order to test the reliability of the VMS on phosphorescence spectra, especially on transition metal complexes which have not been much studied,[9, 10, 22] a computational investigation of the triplet excited state has been performed. As one can see in Figure 3, the GS and ES geometries of complex **2** are almost identical. On the contrary, the ES and GS geometries of complex **3** show some differences, but they remain similar enough to perform on these grounds the vibronic treatment.

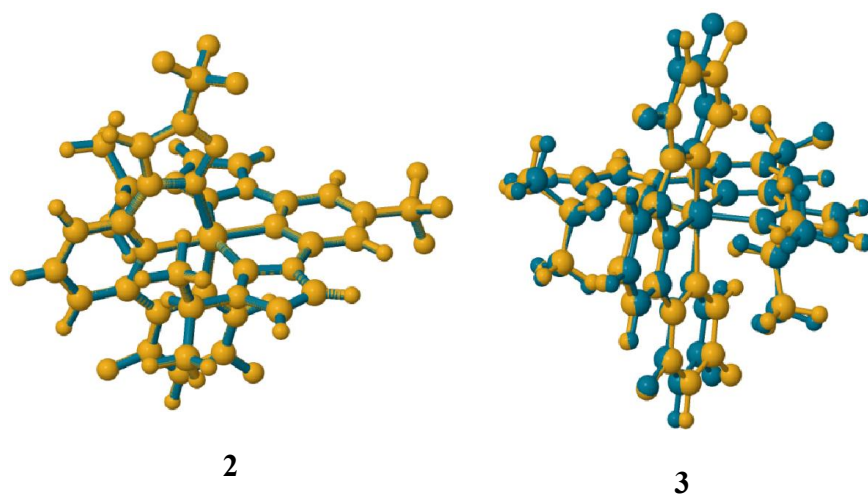


Figure 3. Superimposed GS and ES geometries of complexes **2**(left) and **3**(right).

As one can see in Figure 2b, complexes **3** and **3b** are red shifted with respect to complexes **2** and **2b**. Furthermore, complexes with *PimB* ligand (**2b** and **3b**) also exhibit a red shift in comparison to complexes with *PimF* ligand (**2** and **3**). These trends are nicely reproduced in our simulated spectra (Figure 4). Moreover, the band maxima of experiment and simulations are also in a good agreement despite a small underestimation (less than 50 nm) of the maxima. Finally, it should be mentioned the very good agreement concerning the band shapes. If one compares the spectra of

complexes **2** and **2b**, it is observed three maxima, one shoulder and a long tail. This band structure is perfectly reproduced in our simulations. It turns out that the relative intensities are also well described in the simulations but the absolute intensities remain underestimated, especially for the second maxima. Finally, complexes **3** and **3b** exhibit a structure less emission band centred around 550 nm. This sharp band is also nicely reproduced in the simulation. The emission spectra of complexes **2** and **2b** exhibit several bands contrarily to complexes **3** and **3b**. Considering the MOs involved in the HOMO-LUMO transition (Figure 1) leading to the emitting $^3\text{MLCT}$ excited state of complex **2**, it can be seen a ligand $\pi\text{-}\pi^*$ contribution to the excitation. Moreover, vibration modes of this ligand appear to participate to the vibronic structure of the emission spectrum of complex **2** computed using the adiabatic shift approach (see computational details); these facts are likely to explain the structured phosphorescence spectrum of this complex. On the contrary, such ligand influence on the emission spectrum is not observed for complex **3**.

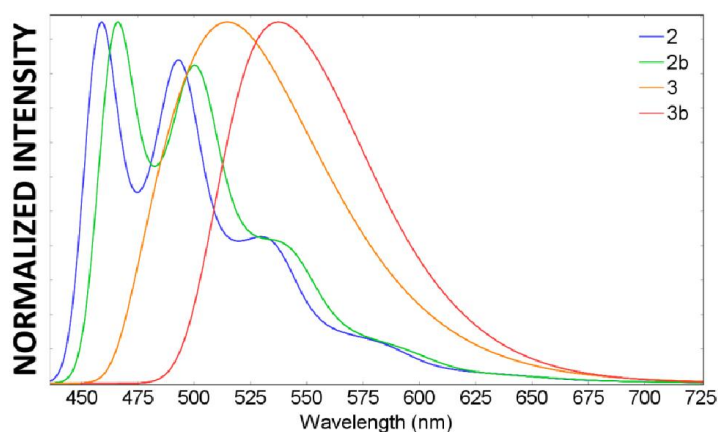


Figure 4. Simulated Phosphorescence Spectra of Complexes **2**, **2b**, **3** and **3b**.

4. Conclusion

In this article we have provided explanations of the optical (absorption and emission) properties of six new iridium complexes using quantum chemistry. Complex **1** does not exhibit luminescence properties in solution and calculations furnish hypotheses of this absence. Contrarily, complexes **2** and **3** have shown a strong phosphorescence signature, which have been nicely reproduced and rationalized in our simulations. Indeed, the simulated phosphorescence spectra using the VMS approach allowed a direct vis-à-vis between experiment and simulations. As recently stated by some authors, the computational protocol to perform excited state investigations on Ir(III) complexes seems to be efficient, *e. g.* B3PW91/LANL2DZ+pol.[9, 10] New investigations using this methodology are by substituting the iridium center by another transition metal.

References

1. D'Andrade BW, Forrest SR (2004) White Organic Light-Emitting Devices for Solid-State Lighting. *Adv Mater* 16:1585–1595. doi: 10.1002/adma.200400684
2. Sun Y, Forrest SR (2007) High-efficiency white organic light emitting devices with three separate phosphorescent emission layers. *Appl Phys Lett* 91:263503. doi: <http://dx.doi.org/10.1063/1.2827178>
3. Chen C-Y, Pootrakulchote N, Chen M-Y, et al (2012) A New Heteroleptic Ruthenium Sensitizer for Transparent Dye-Sensitized Solar Cells. *Adv Energy Mater* 2:1503–1509. doi: 10.1002/aenm.201200285
4. Schulze M, Steffen A, Würthner F (2015) Near-IR Phosphorescent Ruthenium(II) and Iridium(III) Perylene Bisimide Metal Complexes. *Angew Chemie Int Ed* 54:1570–1573.

doi: 10.1002/anie.201410437

5. Angelis F De, Belpassi L, Fantacci S (2009) Spectroscopic properties of cyclometallated iridium complexes by TDDFT. *J Mol Struct THEOCHEM* 914:74–86. doi: <http://dx.doi.org/10.1016/j.theochem.2009.07.025>
6. Dragonetti C, Colombo A, Marinotto D, et al (2014) Functionalized styryl iridium (III) complexes as active second-order NLO chromophores and building blocks for SHG polymeric films. *J Organomet Chem* 751:568–572.
7. Broeckx LEE, Delaunay W, Latouche C, et al (2013) C-H activation of 2,4,6-triphenylphosphinine: synthesis and characterization of the first homoleptic phosphinine-iridium(III) complex fac-[Ir(C^P)₃]. *Inorg Chem* 52:10738–40. doi: 10.1021/ic401933m
8. Sun H, Liu S, Lin W, et al (2014) Smart responsive phosphorescent materials for data recording and security protection. *Nat Commun* 5:3601. doi: 10.1038/ncomms4601
9. Vazart F, Latouche C (2015) Validation of a computational protocol to simulate near IR phosphorescence spectra for Ru(II) and Ir(III) metal complexes. *Theor Chem Acc* 134:1–7. doi: 10.1007/s00214-015-1737-0
10. Latouche C, Skouteris D, Palazzetti F, Barone V (2015) TD-DFT Benchmark on Inorganic Pt(II) and Ir(III) Complexes. *J Chem Theory Comput* 11:3281–3289. doi: 10.1021/acs.jctc.5b00257
11. Heinze K, Hempel K, Tschierlei S, et al (2009) Resonance Raman Studies of Bis(terpyridine)ruthenium(II) Amino Acid Esters and Diesters. *Eur J Inorg Chem* 2009:3119–3126. doi: 10.1002/ejic.200900309
12. Bhuiyan A a., Kincaid JR (1998) Synthesis and Photophysical Properties of Zeolite-Entrapped Bisterpyridine Ruthenium(II). Dramatic Consequences of Ligand-Field-State Destabilization. *Inorg Chem* 37:2525–2530. doi: 10.1021/ic970950u

13. Muhavini Wawire C, Jouvenot D, Loiseau F, et al (2013) Density-functional study of luminescence in polypyridine ruthenium complexes. *J Photochem Photobiol A Chem* 276:8–15. doi: <http://dx.doi.org/10.1016/j.jphotochem.2013.10.018>
14. Bergeron B V, Meyer GJ (2002) Reductive Electron Transfer Quenching of MLCT Excited States Bound To Nanostructured Metal Oxide Thin Films. *J Phys Chem B* 107:245–254. doi: 10.1021/jp026823n
15. Johansson PG, Kopecky A, Galoppini E, Meyer GJ (2013) Distance Dependent Electron Transfer at TiO₂ Interfaces Sensitized with Phenylene Ethynylene Bridged RuII–Isothiocyanate Compounds. *J Am Chem Soc* 135:8331–8341. doi: 10.1021/ja402193f
16. Lundqvist MJ, Galoppini E, Meyer GJ, Persson P (2007) Calculated Optoelectronic Properties of Ruthenium Tris-bipyridine Dyes Containing Oligophenyleneethynylene Rigid Rod Linkers in Different Chemical Environments. *J Phys Chem A* 111:1487–1497. doi: 10.1021/jp064219x
17. Schoonover JR, Bates WD, Meyer TJ (1995) Application of Resonance Raman Spectroscopy to Electronic Structure in Metal Complex Excited States. Excited-State Ordering and Electron Delocalization in Dipyrido[3,2-a:2',3'-c]phenazine (dppz): Complexes of Re(I) and Ru(II). *Inorg Chem* 34:6421–6422. doi: 10.1021/ic00130a004
18. Latouche C, Baiardi A, Barone V (2014) Virtual Eyes Designed for Quantitative Spectroscopy of Inorganic Complexes: Vibronic Signatures in the Phosphorescence Spectra of Terpyridine Derivatives. *J. Phys. Chem. B*
19. Barone V, Biczysko M, Bloino J (2014) Fully anharmonic IR and Raman spectra of medium-size molecular systems: accuracy and interpretation. *Phys Chem Chem Phys* 16:1759–1787. doi: 10.1039/C3CP53413H
20. Biczysko M, Panek P, Scalmani G, et al (2010) Harmonic and Anharmonic Vibrational Frequency Calculations with the Double-Hybrid B2PLYP Method : *J Chem Theory*

- Comput 6:2115–2125.
21. Baiardi A, Bloino J, Barone V (2015) “Accurate simulation of Resonance-Raman spectra of flexible molecules: an internal coordinates approach.” *J Chem Theory Comput* DOI:10.1021/acs.jctc.5b00241. doi: 10.1021/acs.jctc.5b00241
 22. Vazart F, Latouche C, Bloino J, Barone V (2015) Vibronic Coupling Investigation to Compute Phosphorescence Spectra of Pt(II) Complexes. *Inorg Chem* 54:5588–5595. doi: 10.1021/acs.inorgchem.5b00734
 23. Latouche C, Palazzetti F, Skouteris D, Barone V (2014) High-Accuracy Vibrational Computations for Transition Metal Complexes Including Anharmonic Corrections: Ferrocene, Ruthenocene and Osmocene as test cases. *J Chem Theory Comput* 10:4565–4573. doi: 10.1021/ct5006246
 24. Green K, Gauthier N, Sahnoune H, et al (2013) Covalent Immobilization of Redox-Active Fe(κ^2 -dppe)(η^5 -C₅Me₅)-Based π -Conjugated Wires on Oxide-Free Hydrogen-Terminated Silicon Surfaces. *Organometallics* 32:5333–5342. doi: 10.1021/om4006017
 25. Sahnoune H, Baranová Z, Bhuvanesh N, et al (2013) A Metal-Capped Conjugated Polyynes Threaded through a Phenanthroline-Based Macrocyclic. Probing beyond the Mechanical Bond to Interactions in Interlocked Molecular Architectures. *Organometallics* 32:6360–6367. doi: 10.1021/om400709q
 26. Makhoul R, Sahnoune H, Davin T, et al (2014) Proton-Controlled Regioselective Synthesis of [Cp*(dppe)Fe–C \equiv C–1-(η^6 -C₁₀H₇)Ru(η^5 -Cp)](PF₆) and Electron-Driven Haptotropic Rearrangement of the (η^5 -Cp)Ru + Arenophile. *Organometallics* 33:4792–4802. doi: 10.1021/om500047k
 27. Green K, Gauthier N, Sahnoune H, et al (2013) Synthesis and Characterization of Redox-Active Mononuclear Fe(κ^2 -dppe)(η^5 -C₅Me₅)-Terminated π -Conjugated Wires. *Organometallics* 32:4366–4381. doi: 10.1021/om400515g

28. Latouche C, Liu CW, Saillard J-Y (2014) Encapsulating Hydrides and Main-Group Anions in d¹⁰-Metal Clusters Stabilized by 1,1-Dichalcogeno Ligands. *J Clust Sci* 25:147–171. doi: 10.1007/s10876-013-0671-3
29. Liao J-H, Latouche C, Li B, et al (2014) A twelve-coordinated iodide in a cuboctahedral silver(I) skeleton. *Inorg Chem* 53:2260–7. doi: 10.1021/ic402960e
30. Latouche C, Lin Y-R, Tobon Y, et al (2014) Au-Au chemical bonding induced by UV irradiation of dinuclear gold(I) complexes: a computational study with experimental evidence. *Phys Chem Chem Phys* 16:25840–5.
31. Boixel J, Guerchais V, Le Bozec H, et al (2014) Second-Order NLO Switches from Molecules to Polymer Films Based on Photochromic Cyclometalated Platinum(II) Complexes. *J Am Chem Soc* 136:5367–5375. doi: 10.1021/ja4131615
32. Jacquemin D, Perpète EA, Scuseria GE, et al (2008) TD-DFT Performance for the Visible Absorption Spectra of Organic Dyes: Conventional versus Long-Range Hybrids. *J Chem Theory Comput* 4:123–135. doi: 10.1021/ct700187z
33. Steffen A, Costuas K, Boucekkine A, et al (2014) Fluorescence in Rhoda- and Iridacyclopentadienes Neglecting the Spin–Orbit Coupling of the Heavy Atom: The Ligand Dominates. *Inorg Chem* 53:7055–7069. doi: 10.1021/ic501115k
34. Jacquemin D, Perpète EA, Scuseria GE, et al (2008) Extensive TD-DFT investigation of the first electronic transition in substituted azobenzenes. *Chem Phys Lett* 465:226–229. doi: <http://dx.doi.org/10.1016/j.cplett.2008.09.071>
35. Jacquemin D, Preat J, Wathelet V, et al (2006) Thioindigo Dyes: Highly Accurate Visible Spectra with TD-DFT. *J Am Chem Soc* 128:2072–2083. doi: 10.1021/ja056676h
36. Latouche C, Barone V (2014) Computational Chemistry Meets Experiments for Explaining the Behavior of Bibenzyl: A Thermochemical and Spectroscopic (Infrared,

- Raman, and NMR) Investigation. *J Chem Theory Comput* 10:5586–5592. doi: 10.1021/ct500930b
37. Latouche C, Kahlal S, Furet E, et al (2013) Shape Modulation of Octanuclear Cu (I) or Ag (I) Dichalcogeno Template Clusters with Respect to the Nature of their Encapsulated Anions: A Combined Theoretical and Experimental Investigation. *Inorg Chem* 52:7752–7765.
 38. Latouche C, Kahlal S, Lin Y-R, et al (2013) Anion Encapsulation and Geometric Changes in Hepta- and Hexanuclear Copper (I) Dichalcogeno Clusters: A Theoretical and Experimental Investigation. *Inorg Chem* 52:13253–13262.
 39. Latouche C, Lanoe P-H, Williams JAG, et al (2011) Switching of excited states in cyclometalated platinum complexes incorporating pyridyl-acetylide ligands (Pt–C [triple bond, length as m-dash] C–py): a combined experimental and theoretical study. *New J Chem* 35:2196–2202.
 40. Barone V, Latouche C, Skouteris D, et al (2015) Gas-phase formation of the prebiotic molecule formamide: insights from new quantum computations. *Mon Not R Astron Soc Lett* 453:L31–L35.
 41. Vlček A, Zális S (2007) Modeling of charge-transfer transitions and excited states in d6 transition metal complexes by DFT techniques. *Coord Chem Rev* 251:258–287. doi: 10.1016/j.ccr.2006.05.021
 42. Barone V, Baiardi A, Biczysko M, et al (2012) Implementation and validation of a multi-purpose virtual spectrometer for large systems in complex environments. *Phys Chem Chem Phys* 14:12404–12422. doi: 10.1039/C2CP41006K
 43. Licari D, Baiardi A, Biczysko M, et al (2015) Implementation of a graphical user interface for the virtual multifrequency spectrometer: The VMS-Draw tool. *J Comput Chem* 36:321–334.

44. Barone V (2016) The virtual multifrequency spectrometer: a new paradigm for spectroscopy. *Wiley Interdiscip Rev Comput Mol Sci* 6:86–110. doi: 10.1002/wcms.1238
45. Bloino J, Barone V (2012) A second-order perturbation theory route to vibrational averages and transition properties of molecules: General formulation and application to infrared and vibrational circular dichroism spectroscopies. *J Chem Phys* 136:124108. doi: <http://dx.doi.org/10.1063/1.3695210>
46. Barone V (2012) *Computational Strategies for Spectroscopy*. John Wiley & Sons Inc., Hoboken, New Jersey
47. Barone V, Biczysko M, Bloino J, et al (2012) Toward anharmonic computations of vibrational spectra for large molecular systems. *Int J Quantum Chem* 112:2185–2200. doi: 10.1002/qua.23224
48. Piccardo M, Bloino J, Barone V (2015) Generalized vibrational perturbation theory for rovibrational energies of linear, symmetric and asymmetric tops: Theory, approximations, and automated approaches to deal with medium-to-large molecular systems. *Int J Quantum Chem* 115:948–982. doi: 10.1002/qua.24931
49. Egidi F, Bloino J, Barone V, Cappelli C (2012) Toward an Accurate Modeling of Optical Rotation for Solvated Systems: Anharmonic Vibrational Contributions Coupled to the Polarizable Continuum Model. *J Chem Theory Comput* 8:585–597.
50. Baiardi A, Bloino J, Barone V (2013) General Time Dependent Approach to Vibronic Spectroscopy Including Franck–Condon, Herzberg–Teller, and Duschinsky Effects. *J Chem Theory Comput* 9:4097–4115. doi: 10.1021/ct400450k
51. Muniz-Miranda F, Pedone A, Battistelli G, et al (2015) Benchmarking TD-DFT against Vibrationally Resolved Absorption Spectra at Room Temperature: 7-Aminocoumarins as Test Cases. *J Chem Theory Comput* 11:5371–5384. doi: 10.1021/acs.jctc.5b00750

52. Puzzarini C, Biczysko M, Barone V (2010) Accurate Harmonic/Anharmonic Vibrational Frequencies for Open-Shell Systems: Performances of the B3LYP/N07D Model for Semirigid Free Radicals Benchmarked by CCSD(T) Computations. *J Chem Theory Comput* 6:828–838. doi: 10.1021/ct900594h
53. Barone V, Biczysko M, Bloino J, Puzzarini C (2013) Glycine conformers: a never-ending story? *Phys Chem Chem Phys* 15:1358–1363. doi: 10.1039/C2CP43884D
54. Bloino J, Biczysko M, Santoro F, Barone V (2010) General Approach to Compute Vibrationally Resolved One-Photon Electronic Spectra. *J Chem Theory Comput* 6:1256–1274.
55. Barone V, Bloino J, Guido CA, Lipparini F (2010) A fully automated implementation of VPT2 Infrared intensities. *Chem Phys Lett* 496:157–161. doi: <http://dx.doi.org/10.1016/j.cplett.2010.07.012>
56. Biczysko M, Panek P, Scalmani G, et al (2010) Harmonic and Anharmonic Vibrational Frequency Calculations with the Double-Hybrid B2PLYP Method: Analytic Second Derivatives and Benchmark Studies. *J Chem Theory Comput* 6:2115–2125. doi: 10.1021/ct100212p
57. Banerjee S, Baiardi A, Bloino J, Barone V (2016) Vibronic Effects on Rates of Excitation Energy Transfer and Their Temperature Dependence. *J Chem Theory Comput* 12:2357–2365. doi: 10.1021/acs.jctc.6b00157
58. Hodecker M, Biczysko M, Dreuw A, Barone V (2016) Simulation of Vacuum UV Absorption and Electronic Circular Dichroism Spectra of Methyl Oxirane: The Role of Vibrational Effects. *J Chem Theory Comput* 12:2820–2833. doi: 10.1021/acs.jctc.6b00121
59. Frisch MJ, Trucks GW, Schlegel HB, et al Gaussian~09 {R}evision {D}.01.
60. Becke AD (1993) Density functional thermochemistry. III. The role of exact exchange. *J.*

Chem. Phys. 98:

61. Perdew JP (1986) Density-functional approximation for the correlation energy of the inhomogeneous electron gas. *Phys Rev B* 33:8822–8824.
62. Perdew JP, Burke K, Wang Y (1996) Generalized gradient approximation for the exchange-correlation hole of a many-electron system. *Phys Rev B* 54:16533–16539. doi: 10.1103/PhysRevB.54.16533
63. Dunning Jr. TH, Hay PJ (1977) Gaussian Basis Sets for Molecular Calculations. In: Schaefer III H (ed) *Methods Electron. Struct. Theory SE - 1*. Springer US, pp 1–27
64. Hay PJ, Wadt WR (1985) Ab initio effective core potentials for molecular calculations. Potentials for K to Au including the outermost core orbitals. *J. Chem. Phys.* 82:
65. Hay PJ, Wadt WR (1985) Ab initio effective core potentials for molecular calculations. Potentials for the transition metal atoms Sc to Hg. *J. Chem. Phys.* 82:
66. Wadt WR, Hay PJ (1985) Ab initio effective core potentials for molecular calculations. Potentials for main group elements Na to Bi. *J. Chem. Phys.* 82:
67. Cossi M, Scalmani G, Rega N, Barone V (2002) New developments in the polarizable continuum model for quantum mechanical and classical calculations on molecules in solution. *J Chem Phys* 117:43. doi: 10.1063/1.1480445
68. Barone V, Cossi M, Tomasi J (1997) A new definition of cavities for the computation of solvation free energies by the polarizable continuum model. *J. Chem. Phys.* 107:
69. Grimme S, Antony J, Ehrlich S, Krieg H (2010) A consistent and accurate ab initio parametrization of density functional dispersion correction (DFT-D) for the 94 elements H-Pu. *J Chem Phys*. doi: <http://dx.doi.org/10.1063/1.3382344>
70. Barone V, Bloino J, Biczysko M, Santoro F (2009) Fully Integrated Approach to Compute Vibrationally Resolved Optical Spectra: From Small Molecules to Macrosystems. *J Chem*

Theory Comput 5:540–554. doi: 10.1021/ct8004744

71. Dennington, R.; Keith, T.; Millam J (2009) GaussView, Version 5.
72. Gorelsky SI (2009) AOMix: Program for Molecular Orbital Analysis.
73. Gorelsky SI (2009) Swizard.